MODELLING SHALE GAS FLOW USING THE IDEA OF APPARENT DYNAMIC PERMEABILITY

A Thesis

by

SYED MUNIB ULLAH FARID

Submitted to the Office of Graduate and Professional Studies of
Texas A&M University
in partial fulfillment of the requirements for the degree of

MASTER OF SCIENCE

Chair of Committee,	John E. Killough
Committee Members,	Maria. A. Barrufet
	Zoya Heidari
Head of Department,	A. Daniel Hill

May 2015

Major Subject: Petroleum Engineering

ABSTRACT

The basic idea behind this research is to propose a work flow to model gas flow in numerical simulators, which would take into consideration all the complexities of the multiple porosity systems that exist in shale matrix and the different dynamics of flow involved within them. The concept of a multi porosity system that is composed of the organic part (kerogen), inorganic matter, and natural and hydraulic fractures is used here. Kerogen is very different from other shale components because of its highly porous nature, capability to adsorb gas and abundance of nano-pores on its surface.

Some theories have been put forward for the physics involved in shale on a micro scale level. However, when working with reservoir scale models, the details as described for porosity systems in micro scale models is lost. To overcome this problem, the idea of dynamic apparent permeability, which is a function of matrix pressure, is used. It helps in up-scaling the particulars of the micro scale model to a reservoir one and aids in modelling Darcy flow, Fickian diffusion and transition flow in between the matrix and fractures.

Our assumptions are validated by working with the case of a horizontal well model, producing gas from the Barnett shale formation, that doesn't take into consideration the relevant flow phenomenon. History matching the model after integrating diffusion and desorption reveals that considering these additional processes impacts the assumed SRV region, affecting its volume as well as its properties. This would be a critical factor in

optimizing completion design, to lower down the well cost for same or ever greater production. Similarly, this can play a vital role in well spacing for effective field development.

We summarize our findings from production forecasts that matrix contribution towards production is under estimated when relevant assumptions for shale are not modelled. This signifies the importance of better understating the transport phenomenon occurring in shale, which would enable us to have a greater insight to scrutinize production data and later to predict changes in production as completion methods are changed. This means that a multi stage high density fracturing job might not optimize the well in terms of its value. Decreasing our expenditure on well completions, such that their design results in lower production rates at the initial time period along with lower decline rates, would enable us to produce these wells longer for the same recovery. This would enable us to push the production in future where oil and gas prices might be better.

DEDICATION

I dedicate this work to the beautiful spirit of people, all around the world.

ACKNOWLEDGEMENTS

I would like to especially thank my advisor Prof. John E Killough who encouraged and helped me throughout this project. His insightful implementations of the ideas led to many important improvements. Without his guidance and patience, this work would have never materialized.

I would also like to thank Institute of International Education (IIE) and US State Department of Educational and Cultural Affairs for providing me with an opportunity to work and learn with one of the finest professors of the industry at Harold Vance Department of Petroleum Engineering at Texas A&M. In addition to the financial support, the advice and mentorship provided by the Fulbright advisors at IIE throughout the duration of my stay was invaluable.

I especially wish to thank Dr. Zoya Heidari and Dr. Maria A Barrufet for agreeing to serve on my committee.

I also want to thank my research group members and friends for their support and suggestions. They were often the people to provide initial feedback or suggest improvements whenever I got stuck.

Finally I wish to express my gratitude to my parents who encouraged me at each step and helped me throughout my entire course of study. Their emotional support meant the world at times. My siblings also provided deep moral support and encouragement.

NOMENCLATURE

BHP	Bottom Hole Pressure, Psi
Cg	Gas compressibility, 1/Psi
D	Gas diffusion coefficient, ft^2/second
d_{mf}	Nodal distance between matrix bulk & fracture system in micro model, ft
Kapp	Apparent Permeability within matrix, mD
P	Block pressure, Psi
P_f	Average pressure in the fracture, Psi
P_L	Langmuir pressure which is pressure at $V_L/2$, Psi
P_m	Average pressure in the matrix, Psi
q_a	Mass of gas adsorbed on unit volume of media, lbs/scf
q_{mf}	Total flow rate from matrix into fracture system, scf/sec
Ro	Vitrinite Reflectance
S_g	Saturation of gas, %
S_w	Saturation of water, %
TOC	Total Organic Content (wt %)
Va	amount of gas adsorbed by one ton of rock, scf/lbm

V_L	Langmuir Volume which represents the maximum sorption Capacity, scf/lbm
WHP	Wel Head Pressure, Psi
$\sum A_{mf}$	Total contact area between the matrix bulk and the fracture system, ft^2
$\boldsymbol{\phi}$	Porosity, dimensionless
ρ_g	Gas density, lbm/scf
ρ_s	Skeleton density of the porous media, lbm/scf
$\bar{\mu}_{mf}$	Average gas viscosity in the micro scale model, Pa-second

TABLE OF CONTENTS

Page

LIST OF FIGURES

Page

LIST OF TABLES

Page

CHAPTER I

INTRODUCTION

1.1 Problem Statement

In recent times, we have seen a sharp drop in oil and gas prices, as shown in figure 1. This volatility in fuel prices has resulted in lower rig count this year, especially in United States. The focus of Exploration and Production companies, working in unconventional plays, right now is keeping their production stable, bringing the completion costs down and increasing the accuracy in estimating technically recoverably hydrocarbon volume. This results in fewer wells being drilled, causing the reservoir engineers to work with even lower margin of error while doing the forecast for production. Thus, raising the need of properly understanding the transport phenomenon in Shale formations.

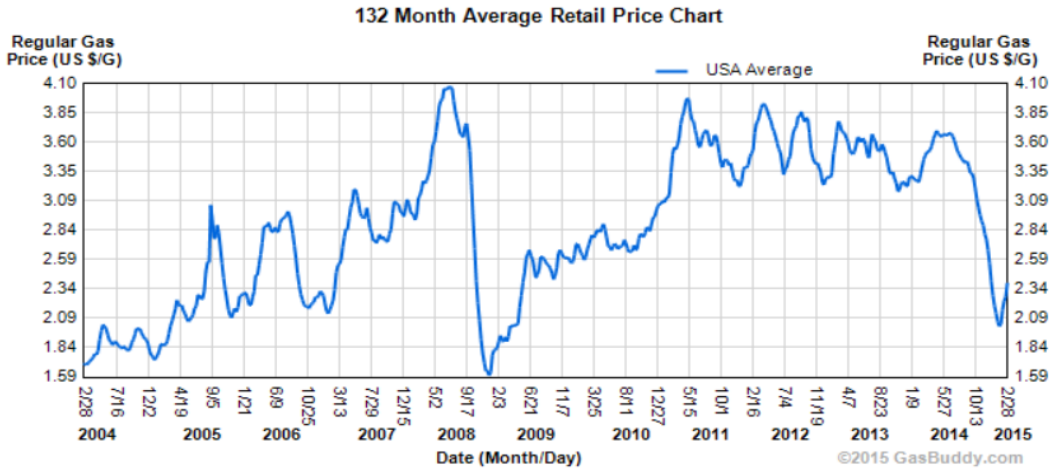

Figure 1 Gas prices in United States for the past 10 years.

Shale gas refers to gas entrapped in fine grained sedimentary rocks, usually called mud-rocks, which can be good source of oil and natural gas. Determining reservoir properties like permeability and predicting gas production from shale strata is important for economic assessments prior to field development. Various theories have been put forward regarding the gas flow in shale formations, but the predictions are usually not accurate and the production is usually higher than the predictions made with Darcy law. Recently, advancements in pore scale characterization, using Focused Ion Beam Spectron Electron Microscopy, have helped in a better understanding of shale morphology. Taking the petro physical perspective for fluid flow in shale, quad porosity systems for gas flow comprising of organic matter, inorganic part, and natural and hydraulic fractures need to be considered (Wang and Reed 2009). Gas is stored as free compressed gas in open pores and cracks, desorbed gas in clays and kerogen surfaces, and as diffused gas in solid organic matter (Sondergeld *et al* 2010). Trying to properly model the transport phenomenon in these systems has always been a challenging problem in reservoir simulation.

The predominant nano-pore system existing in the shale organic matrix has the capability to adsorb gas on its surface along with the free gas that exists in these pores. With the pore system ranging from 5-1000nm and the size of the methane molecule at 0.38 nm, the Klinkenberg effect comes into play. Thus, affecting the gas permeability as a function of reciprocal of mean pressure (specifically at lower pressures). Klinkenberg introduces a slippage factor that is for the condition where the mean free path of gas molecule becomes comparable to the pore throat radii, causing the molecules to slip on the surface. In addition to slippage flow, diffusion also causes deviation from the basic Darcy law.

Currently, dual porosity and permeability systems that discretize the model into matrix and fractures are used for describing these transport phenomenon. These models are governed by the Darcy law. The matrix block is responsible for holding the major chunk of the hydrocarbons while the fractures aid in the transportation of fluid to wellbore because of a pressure difference. However, this technique does not take into consideration the extensive nano and micro-pore system that exists in the kerogens or processes like diffusion and desorption that govern flow within them. Hence, variation in results occur in between the simulation and production data.

In order to tackle this problem, a quad porosity model was proposed (Yan *et al* 2013) that described the physical processes in the different pore systems and how they are connected to each other. However the idea was on a micro scale model that involved dividing the matrix into millions of grid blocks to properly incorporate the details. But these physics are almost lost when scale is changed to reservoir scale model. Additionally, the idea relating the fluid storage and flow in shale gas reservoirs needs to be portable so that it can easily be incorporated to commercial reservoir simulators.

1.2 Background and Literature Review

As advancements are being made with the evolution of the argon milling surface techniques and the field spectron electron microscopy (SEM), imaging of pores as small as 5nm is possible. This helped in classifying pores in shale into those associated with organic matter, whose development is dependent upon thermal maturity. The other type of (non-organic) pores are inter and intra particle which are developed as a result of mechanical and chemical diagenesis. Classification is shown in figure 2.

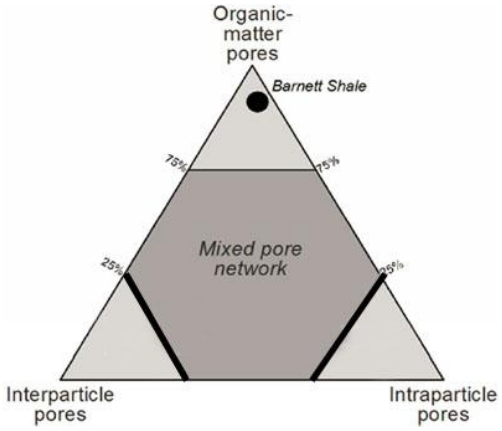

Figure 2 - Identification of matrix pores by the volume percentage of pore network in mud rock systems. Relative proportions of the matrix pore types from Barnett Shale are shown on the ternary diagram.

They occur in between grains and crystal and in between the boundaries of grain respectively. This system of pores is then over-written by a network of fractures that

creates a dual porosity system. A better understanding of the spectrum of different pore sizes helps us in understanding the flow and storage of free gas in mud rock system. A pore network is characterized by a particular pore system if it comprises of 5% by volume or more of the pore network. As can be observed in the ternary diagram, Barnett Shale is dominated by pores in organic matter (Loucks *et al* 2012).

Through high pressure mercury tests on a number of samples, F.Javadpour *et al* (2007) showed the dominance of nano-pores in shale and how they contribute to the evolution of gas. For flow through these nano and micro pore network, conventional laws like Darcy breaks down and Knudsen flow, which is negligible for flow through large pores, becomes important. F.Javadpour *et al* (2009) later proposed a model based on Knudsen diffusion and no slip flow condition. Ertekin *et al* (1986) proposed a dual mechanism approach for Klinkenberg affect by assuming a dynamic gas slippage factor for gas flow in low permeability porous formations. He assumed that gas was flowing under the influence of both macroscopic (pressure) and microscopic (concentration) fields. Flow through pressure field was obeyed through Darcy's law, corrected by Klinkenberg equation which includes a correction factor for gas slippage along the pore walls. Flow in concentration field was followed by Fick's Diffusion law. Since the mean free path of flow of gas molecules is very close to the radii of nano pores they are flowing in, the slip condition in diffusion would be modelled by the Knudsen equation. This is explained in figure 3.

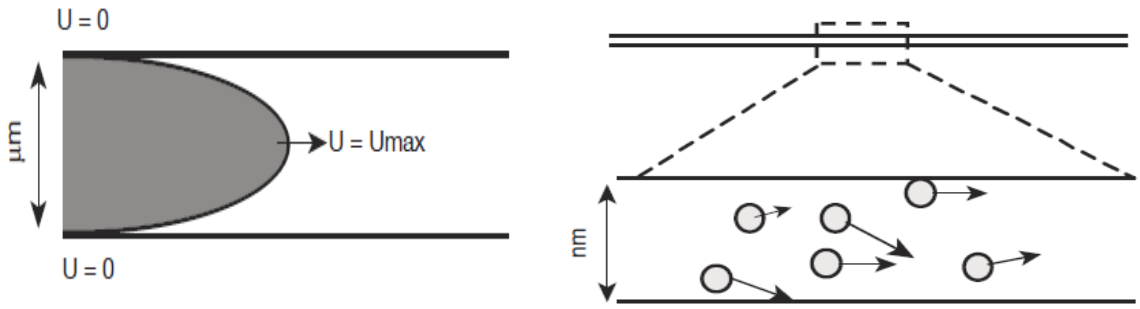

Figure 3 - Comparison of Gas Flow in micro pores where the gas flow is no slip and in nano pores where the flow is slip (Javadpour *et al* 2007).

Most of the work in petroleum engineering literature focusses on the improved efficiency of multi stage hydraulic fracturing, completion and estimation of stimulated reservoir volume (SRV) and their conclusions for history match analysis are focused on mostly different completion strategies. However, there are other factors that may explain the unexpectedly high ultimate recovery from shale plays (Haghshenas etal 2013).

Due to its low porosity and permeability, it takes longer for the gas to flow from the matrix to fracture in shale. Dual permeability models transient very poorly, as it assumes a pseudo steady state for matrix to fracture flow and it is like trying to model the shale matrix explicitly using a single block. The multiple interacting continua (MINC) cannot model matrix to matrix flow, which might not be as important for low permeability shale. But

using LGR's to model hydraulic fractures would not be possible in MINC. These are explained in figure 4.

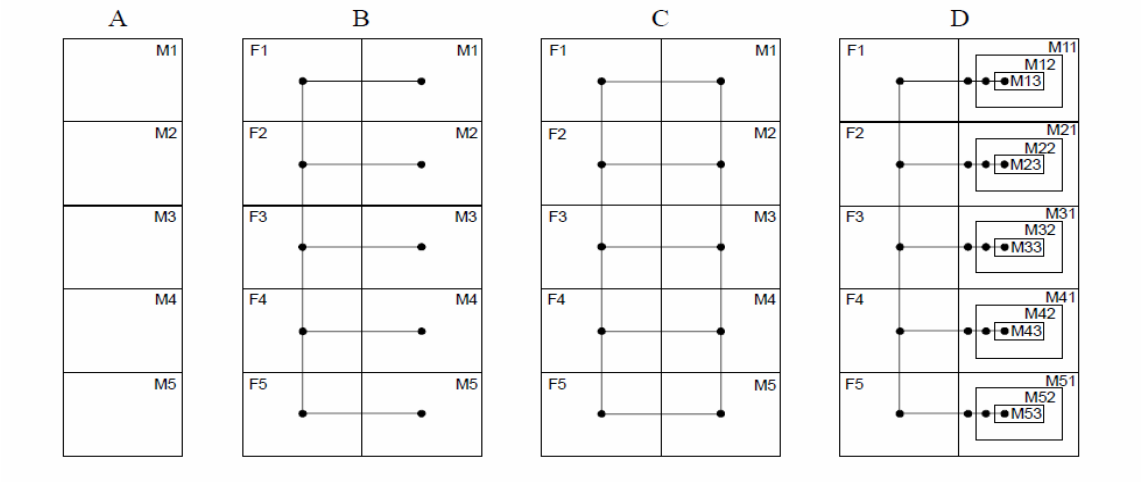

Figure 4 - a) Single Porosity b) Dual Porosity c) Dual Permeability d) Multiple Interacting Continua (CMG Manual 2013)

Yan *et al* (2013) commented that conventional dual porosity/permeability models were incapable of handling the dynamics of flow in nano and micro pore network that exist predominantly in the organic part. He suggested a micro scale multiple porosity model, which divided the shale matrix into organic, inorganic and natural fracture part. This is shown in figure 5. Studies from petro-physical data found that smaller pores in kerogens can be found on the walls of larger pores (Curtis *et al* 2010) – therefore he said that nano pores in organic grids are only connected to the vugs network in organic part and any other porosity system would communicate through these vugs with the organic part. The desorption was supposed to occur only in the kerogen part and this helped in increasing

the TOC in the matrix. The flow form nano to vugs grid was only possible through diffusion, since Darcy law broke down because of small pore size, based on Knudsen number. From vugs to fracture network, flow was guided by both Fickian Diffusion and Darcy's Law whereas the flow in rest of the fracture network was guided by Darcy law.

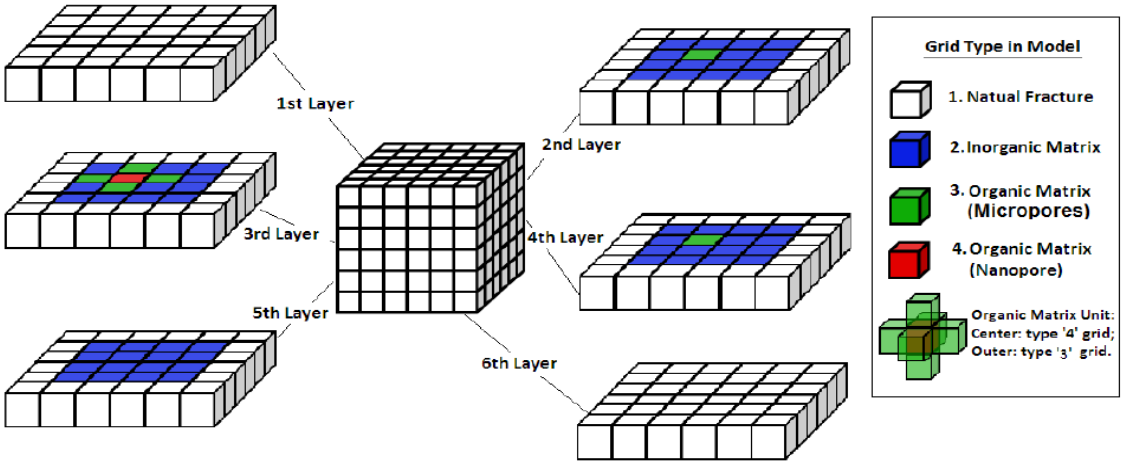

Figure 5 - Schematic of Micro Scale Porosity Mode grid system as proposed by Yan *et al* (2013)

Inorder to make this idea feasible to reservoir scale, he gave the idea of apparent permeability that varied with matrix pressure and was also depedent upon matrix permeability, Darcy flow and diffusion. He made various simulations on reservoir model having a range of static matrix permeabilities.His results showed that a triple permeability model (allowing flow in between natural/hydraulic fractures, organic and inorganic part) would be properly able to model gas flow in shale, provided the dynamic apparent permeability for matrix is integrated into the model. Later on, Yan *et al* (2013) proposed a new definition for apparent permeability that included a coefficient considering the interaction between matrix and fracture. Using it , they proposed that the micro scale model can be upscaled using the variable apparent matrix permeability ratio. But all of this work was observed for a single phase system for gas.

1.3 Objectives and Procedures

Following up on the work done on micro scale models mentioned before, *we are basically trying to bring practical aspects into unconventional by working on field scale*. We tie up the ideas of motion at nano-scale to our results. In this research, a numerical simulator is used to study the effects of different pore configurations and multi storage and flow mechanisms on the production of gas from shale reservoirs, using fundamental physical principles. This is illustrated in figure 6.

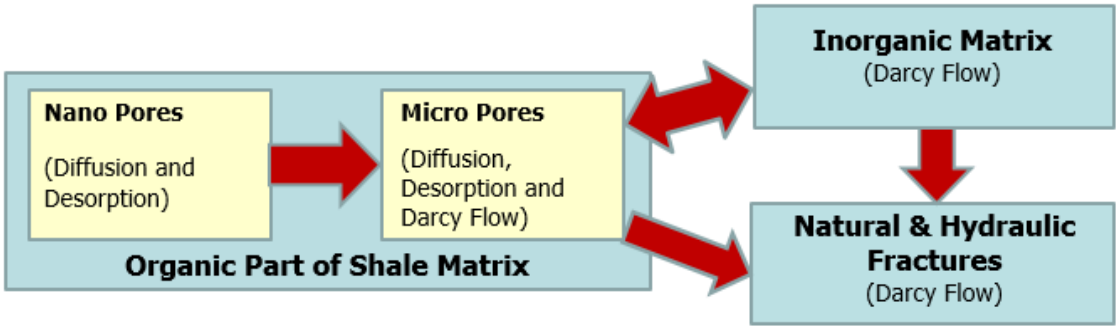

Figure 6 - Basic representation of the assumptions we have made for the shale reservoir model.

- Our initial reservoir model consists of a hydraulically fractured well producing in the Barnett formation, which would be history matched with production data and set up as the base case.
- The shale matrix grid blocks are conceptually divided into organic and inorganic parts, connected to the well bore through a fracture network. The uncertainty associated with the mapping and extent of hydraulically propagated fracture network is kept low, by using observed data from micro-seismic survey.
- Since the organic part in shale plays an important role in gas storage and flow, we would assume it to be composed of both micro-pores (average pore radius: 100 nm) and nano-pores (average pore radius: 5 nm).
- The Total Organic Content value would represent the organic matter dispersed in shale and would impact our simulation results. We would link the value of TOC to Langmuir Volume using relevant correlations. Desorption process would then

be modelled by considering the Langmuir Isotherm. A sensitivity analysis would be performed to show how the TOC values affect the magnitude of the production and reservoir pressures.

- The concept of dynamic apparent permeability is considered for our model to incorporate the effects of different mechanisms like Fickian diffusion, Darcy flow and transient effect between matrix and fracture. This would then enable us to model the relevant flow dynamics in any numerical simulator using rock compressibility tables, giving portability to the idea.
- After incorporating both diffusion and desorption, we would perform a history match to see how these flow mechanisms have impacted the volume and parameters of the SRV region. Finally, forecast would be made using the updated model to see the differences in production and average reservoir pressure over time.

The workflow is summarized in figure 7.

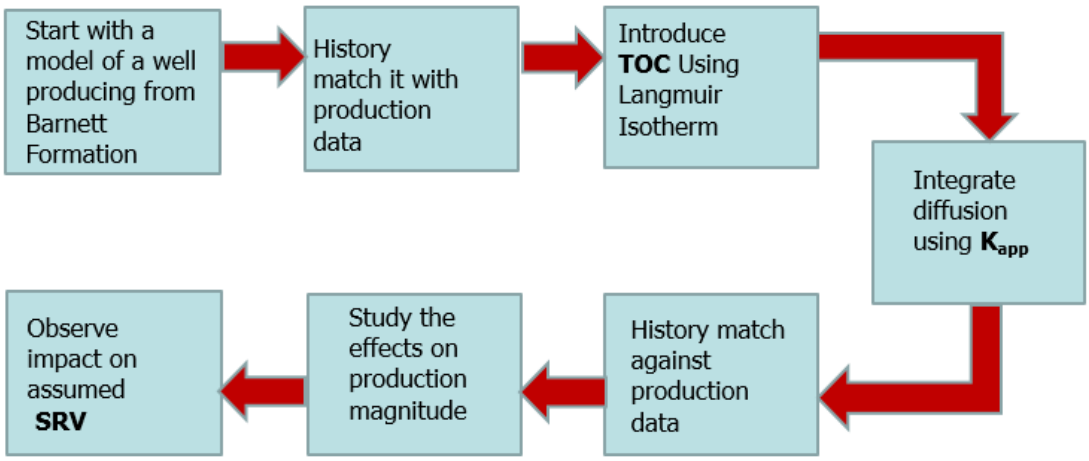

Figure 7- Workflow representing the methodolgy we would be adopting to bring the assumtions of micro scale model to our reservoir scale model.

This study would help to emphasize on the idea of better understanding of the physical phenomenon occurring downhole. It will enable us to have a greater insight when analyzing production data and help in improving engineering tools like reservoir simulators for forecasting changes in production behavior as completion methods are changed.

1.4 Organization of the Thesis

The thesis has been divided into 5 chapters, details of which are as under:

Chapter I introduces us to the basic problem of modelling gas flow in Shale reservoirs porous media. We are given a brief overview of the theories that have been proposed and

how they sort of lack the capability to capture the details. We then define how we would approach this problem and our methodology in proposing a correct solution.

Chapter II gives us the details of the reservoir model we would be working with and the production data we have for that particular well. Relevant equations governing the flow are highlighted.

Chapter III underlines the approach for modelling desorption process and how that mechanism would be impacting our results.

Chapter IV brief us on integrating diffusion and provides us an insight about apparent dynamic permeability and how it varies from Darcy permeability at low reservoir pressures.

Chapter V basically uses the ideas that we discussed in previous chapters and applies it to the model. We then study the changes in production patterns and resulting impact on the SRV region when doing a history match.

Chapter VI presents the conclusions and discusses the important highlights of the study.

CHAPTER II
MODEL DEVELOPMENT

2.1 Physical Model

Barnett shale is one of the most well produced unconventional regions in USA, with majority of wells spread around the Ft. Worth city of North Texas. The Barnett is a Mississippian aged organic rich shale, having the unique characteristic that it serves as its own source, reservoir as well as the seal (Montgomery *et al* 2005). This particular well is located at Newark East field where the formation thickness varies from 300–500 ft. It exhibits mild overpressure (0.52 psi/ft) and about 75% gas saturation at depths of 6500–8500 ft. Geographical map of that area is shown in figure 8.

We start off with a single porosity model of a horizontal well producing in the Barnett Shale, at a depth of 7000 ft using a black oil numerical reservoir simulator (CMG-IMEX). The original well is fracture-stimulated with a large light-sand fracture treatment resulting in a system of linear fractures perpendicular to both fracture principal directions (NE- SW and NW-SE). The fractures were mapped using micro seismic data (Mayerhofer *et al* 2006), which showed that the fracture network was generated with the azimuth mainly in the North Eastern direction along with a component orthogonal to that direction.

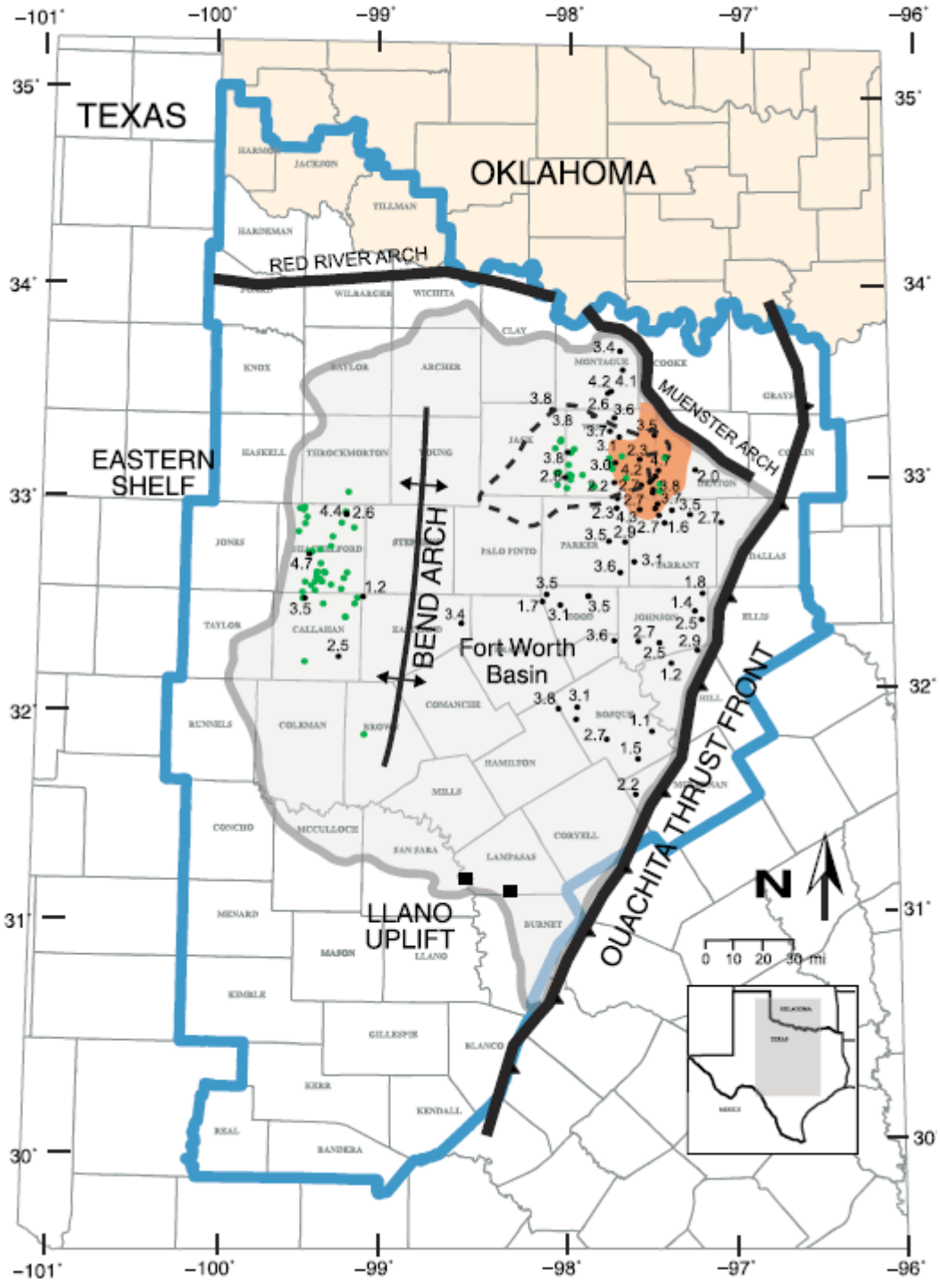

Figure 8 - Map shows the area of US Geological Survey (USGS) Bend Arch – Forth Worth Province 45, with marked location of Newark east field. Location of wells sampled for Total Organic Content are also shown on top.

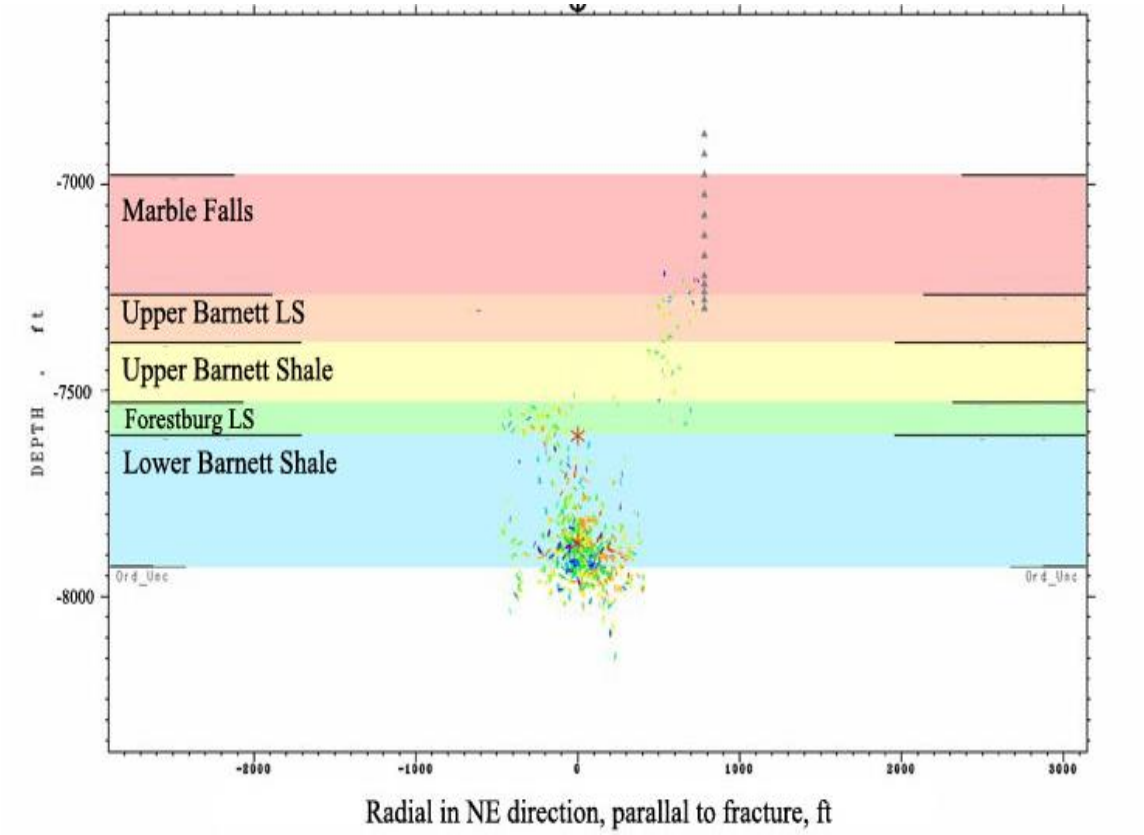

Figure 9 - A side view of the evolution of the fracture network over time in lower Barnett formation

The total extent of the fracture network is 3000 ft, with 3 fracture wings extending to the south west direction, as shown in figure 9. However, the network did not develop as fully in the north east side direction. The network width is around 350 ft and the network height shows that it cover the lower Barnett shale area well, with some traces of the fracture network in upper Barnett formation. This data, comprising of $219*10^6$ scf micro seismically mapped dots, helps us in reducing a reasonable amount of uncertainty with the

mapping of fracture network downhole. The shape of fracture network is shown in figure 10.

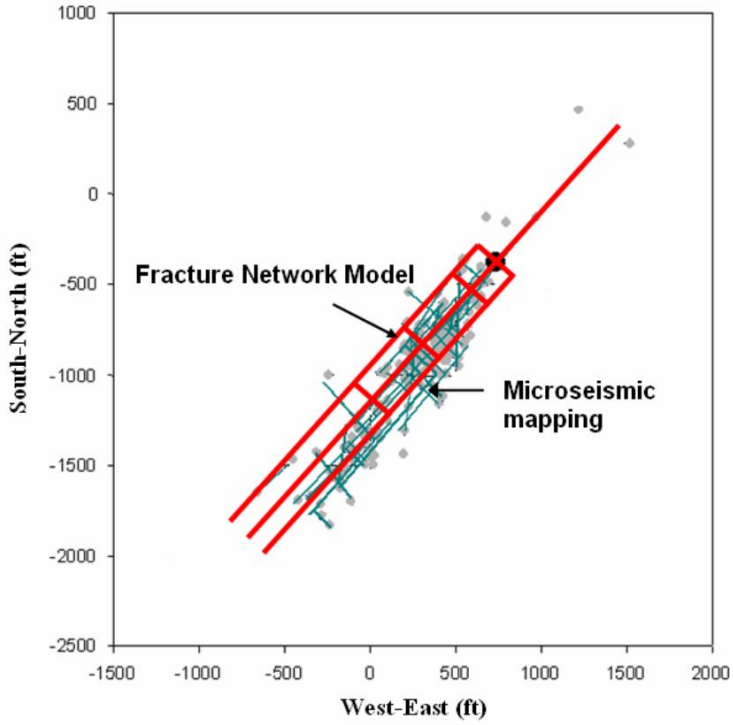

Figure 10 - Shape of fracture network that was determined from seismic data is shown mapped as solid red lines

The model is a Gas-Water fluid system. The dimension of the SRV is 3200 x 660 x 450 scf, represented by 111 x 145 x 1 grid. A 3D representation of our model is shown in figure 11. Two different set of fracture network exists in the system that depicts hydraulic and natural fractures. The fracture width throughout the model is 0.1 ft. Different rock types,

relative permeability curves and compaction tables/values were assigned to the matrix and fractures. The well is produced for around 8 years with constant rate production constraint.

The simulation *does not* include fracturing fluid cleanup, gas desorption or diffusion at this point.

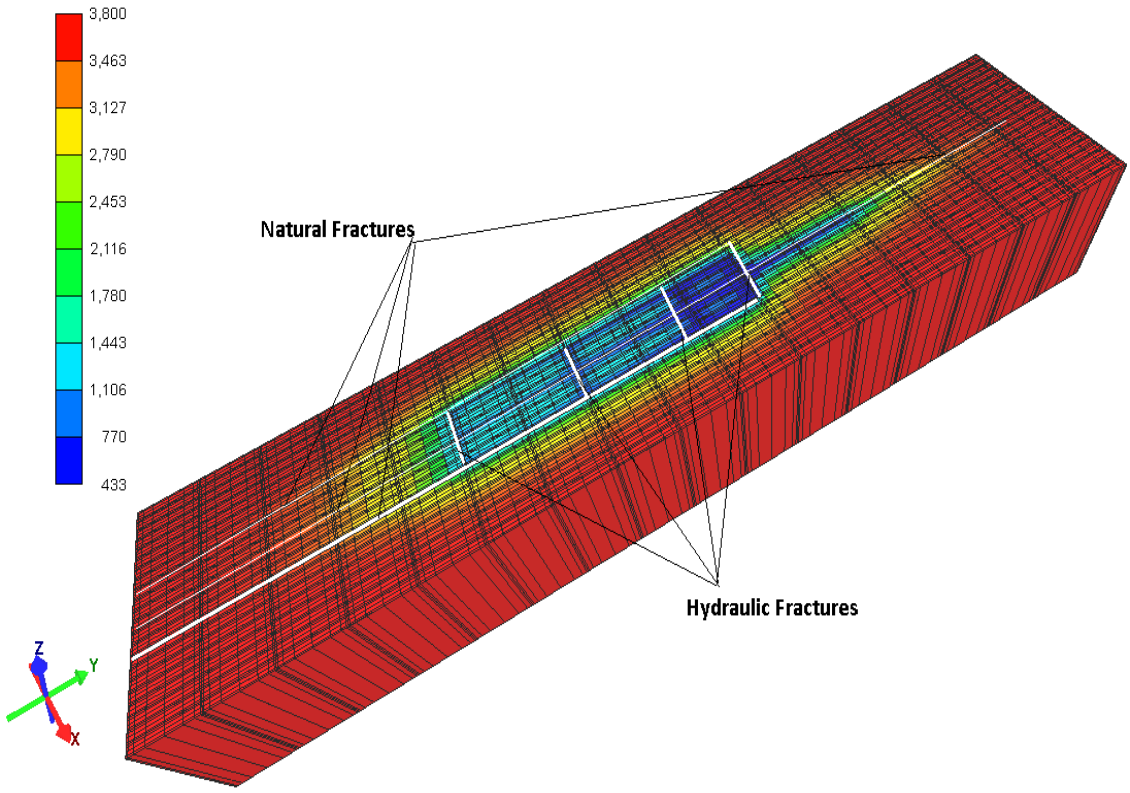

Figure 11 - Pressure Profile for the reservoir model at the end of simulation run for the duration of 8 years. The fracture network is marked from the micro- seismic data that was available.

2.2 History Matching the Model Against Production Data

The original model we had was history matched for the first 4 years (2001/7/2 - 2005/4/25), while we had the production data for 8 years (2001/7/2 - 2008/8/15). The production data consisted of gas production rates (scf/day), well head pressure (psi) and the water produced (bbls/day). As can be seen in figures 9-12, the extension of the duration after the 4 year period did not show a match.

So our first step was to update the base model so that it can be history matched against the entire duration of the field production data. Around 1500 runs were made for this purpose and a number of reservoir parameters were varied, sensitivity analysis of which are shown in the tornado plot attached in Appendix A. Details of the reservoir parameters are mentioned in table 1 below.

Table 1 Reservoir parameters for the base reservoir model of a horizontal well producing in the Barnett Shale formation.

Media Parameters	**Matrix System**	**Fracture Network**		
		Hydraulic	**Natural**	
			Set 1	**Set 2**
Permeability (mD)	0.0001	128	1	57
k_v / k_h Ratio	100	1		
Porosity, %	6.75	70	48	80
Initial Water Saturation, %	30	60		
Relative Permeability Curve Tables *	1	2		
Rock Compaction (1/psi)	3.4E-7 (constant rock compressibility)	3E-6 (Defined by Rock Compaction Table)		
Initial Pressure (psi)	3800			
Temperature (Deg F)	180			
Gas Gravity	0.6			
Depth (ft)	7000			
Net Thickness (ft)	415			

*Attached in Appendix

Figures 12-15 attached below show match of the history match against the results obtained from the initial model.

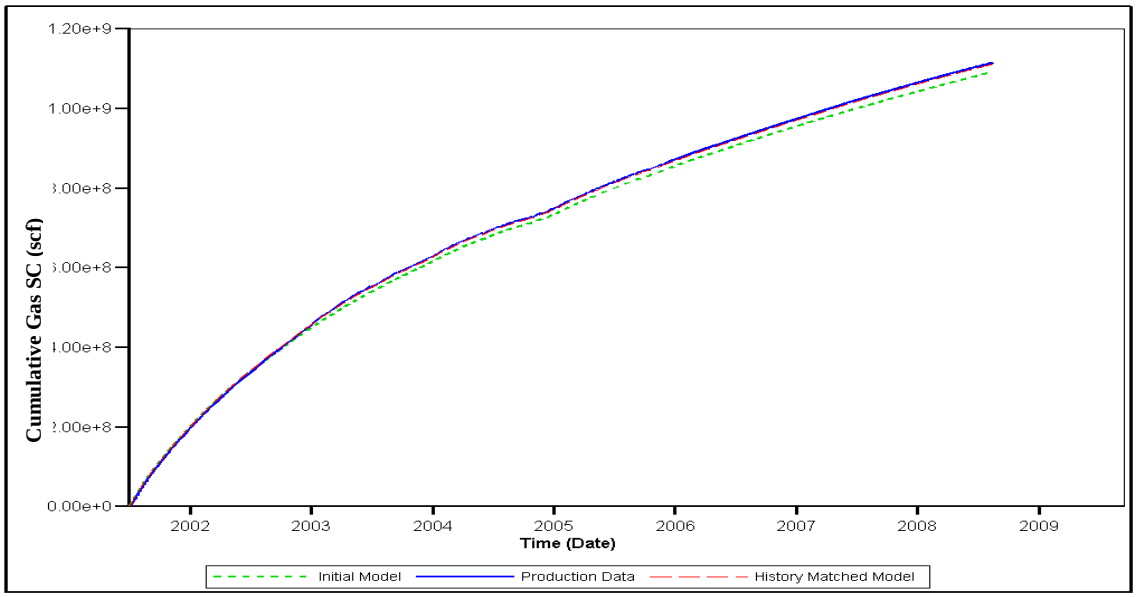

Figure 12 - Cumulative Gas Production for the history matched model against the field production data.

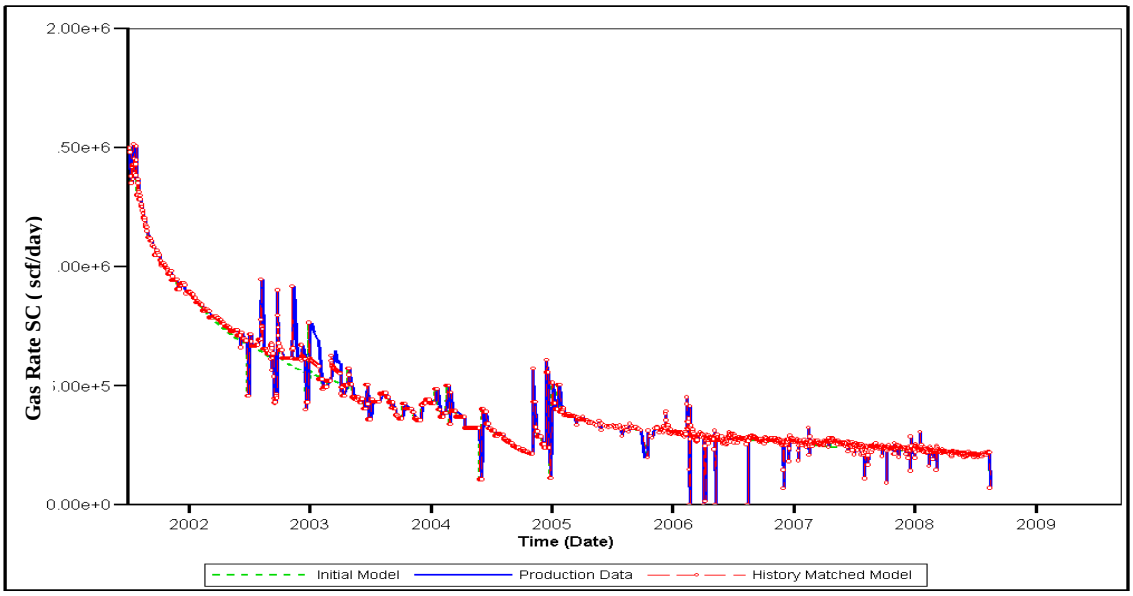

Figure 13- Gas Rate at Surface Condition for the model against the field production data.

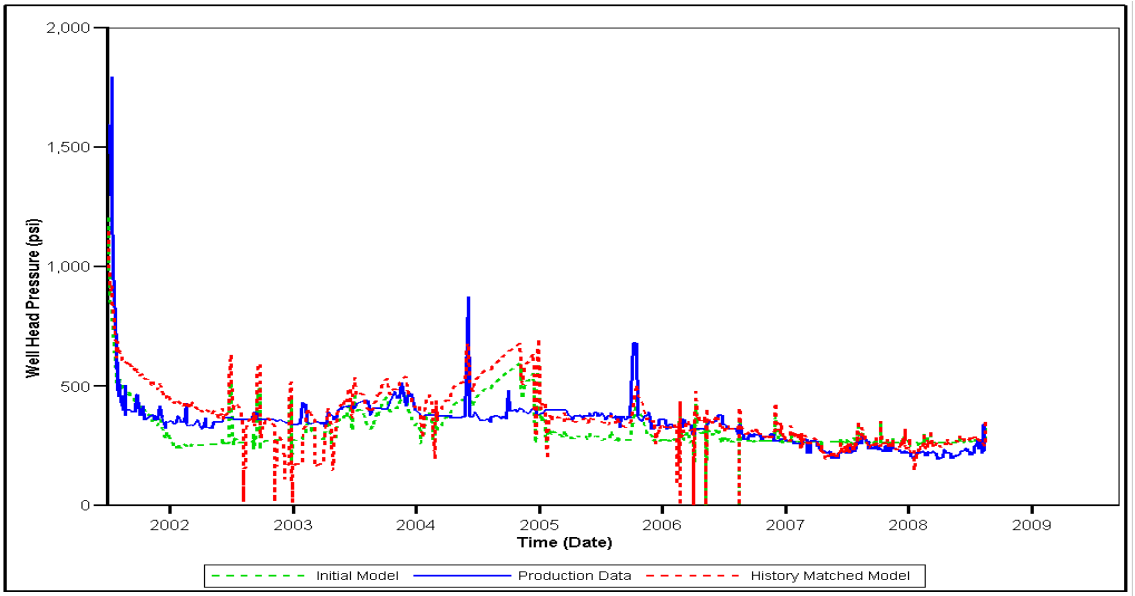

Figure 14 - Well Head Pressure for the history matched model against the field production data.

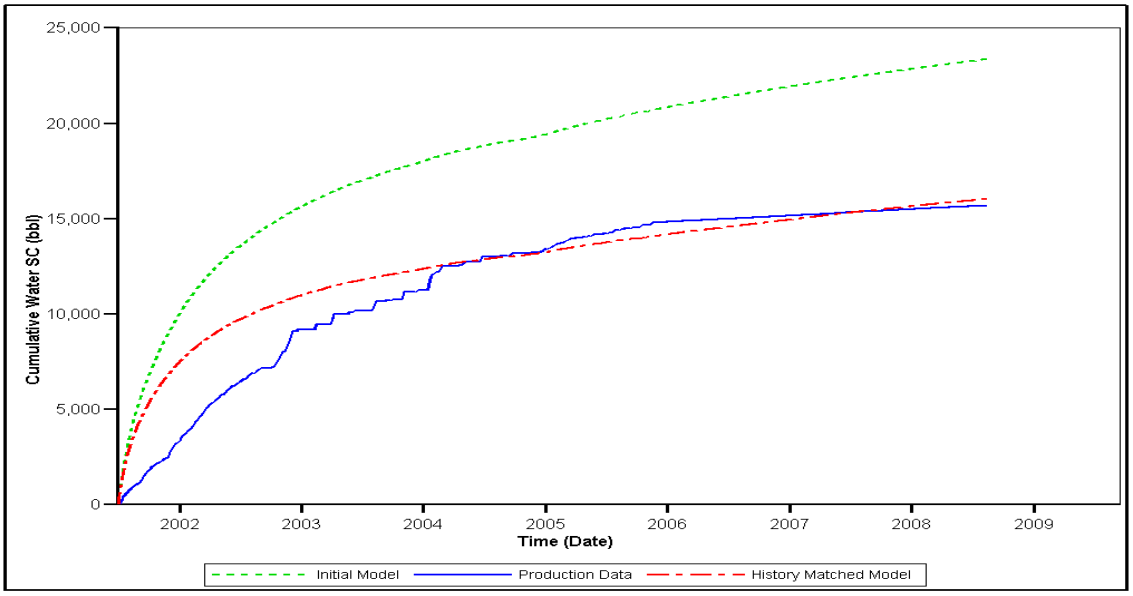

Figure 15 - Cumulative Water Production at Surface Condition for the history matched model against the field production data.

Figure 13 showing gas rates at surface conditions is a signature production profile for shale, where we see large initial production followed by a steep decline. Within a year, the rates falls down to approximately 50% of the rates during the first few days of production. The higher initial production is mainly due to fluid flow in the fracture system.

A histogram of daily water production is attached in appendix A. We can easily observe the fact that in the later time of the production, the data is hardly reported twice a week. Hence, it is not entirely reliable and we didn't put too much weightage on it in the objective function for our history match.

One advantage of matching the model against actual field data would be to clearly understand the impact of desorption and diffusion on our results. We can than do a sensitivity analysis to see how parameters like TOC and permeability multiplier tables affect our cumulative production and pressure drawdown profiles.

2.3 Mathematical Model

We assumed four porosity systems existing in the shale matrix – the micro and nano pores in the organic part with relatively high porosity, the inorganic matrix part with low porosity and these being surrounded by fracture systems that allows pathway to the wellbore through the hydraulic fracture.

Among these continua, the free compressed gas is assumed to be a storage mechanism only in the inorganic mineral part and the fracture network. Gas desorption is supposedly

occurring in the kerogen i-e the organic part. Adsorbed gas molecules increase the original gas in place reserves in the kerogen part. As pressure drawdown is applied, these molecules desorb from the surface. The whole process is modelled using the Langmuir isotherm, which basically relates the adsorption of mono layer gas molecules to pressure or concentration on a solid surface at a particular temperature. It has two fitting parameters: V_L and P_L.

The Langmuir equation is given by

$$\mathbf{q_a = \rho_s \,.\, \rho_g \,.\, V_a} \tag{1}$$

$$\mathbf{V_a} = \frac{\boldsymbol{V_L.P}}{\boldsymbol{P+P_L}} \tag{2}$$

Previously, this work was done using a technique proposed by Seldle *et al* (1990) which used a black oil model's solution gas oil ratio to replicate Langmuir isotherm.

For the flow in between the nano-pore systems, it was assumed that the Darcy flow ceases to exist because the size of gas molecules becomes almost equal to the size of nano-pore radii. It was based on the assumption of Knudsen number, which defines different flow regimes. Therefore, we assume that free and adsorbed gas in nano systems of organic part flows under the Ficks Diffusion law – which is driven by the concentration gradient in between two points. The flow from micro-system to fractures is governed by both Darcy flow and Fickian diffusion. Whereas, there is only Darcy flow for the rest of the system.

We assume that the water molecules occur only in the aqueous phase, in the large pores of the inorganic matrix, while the hydrocarbon molecules exist in the gaseous phase. The solubility of hydrocarbons in the aqueous phase is considered negligible in this model. Therefore the gas phase mass balance and aqueous phase mass balance can be used for the hydrocarbon and gas component respectively, under the assumption of isothermal conditions.

Gas Phase:

$$\nabla.\left[\rho_g\left[DC_g\nabla P+\frac{KK_{rg}}{\mu_g}(\nabla P_g+\rho_g g\nabla z)\right]\right]=-\frac{\partial(\rho_g S_g\varphi)}{\partial t}-\frac{\partial(qa(1-\varphi))}{\partial t} \quad (3)$$

Aqueous Phase:

$$\nabla.\left[\rho_w\left[+\frac{KK_{rw}}{\mu_w}(\nabla P_w+\rho_w g\nabla z)\right]\right]=-\frac{\partial(\rho_w S_w\varphi)}{\partial t} \quad (4)$$

Where $S_w + S_g = 1$

The term on LHS for gas phase refers to the mass flux, into and out of the system. Mass transfer in gaseous phase occurs either due to the Fickian diffusion or Darcy law, or both mechanisms occurring simultaneously depending upon which part of the porosity system you are modelling. For the aqueous phase, we neglect the diffusive term because its affect for liquid is negligible as compared to Darcy law. The RHS terms reflect the accumulation of free compressed gas in all parts of the system and desorbed gas in the organic part.

However, we won't explicitly be using Ficks second law of diffusion here in our model. Instead, we would use the idea of dynamic apparent permeability that was proposed by

Yan *et al* (2010). K_{app} is similar to the Darcian permeability, but is computed as a function of matrix pressure and incorporates different mechanisms, including diffusion, Darcy flow and transition flow in between matrix and fractures, which were coupled in the micro scale model.

$$\mathbf{K_{app}} = \frac{\mathbf{q_f . d_{mf} . \mu_{mf}}}{(P_m - P_f) . \mathbf{\Sigma A_{mf}}} \quad (5)$$

2.4 Conclusion

The details of a reservoir model for a well producing in Barnett shale is presented in this chapter. We describe how the matrix is supposedly divided into organic and inorganic part. These are surrounded by a network of fractures, which have been mapped using micro seismic data.

CHAPTER III

INTEGRATING DESORPTION IN MODEL

3.1 Adsorption Models for Shale Gas Reservoirs

The differentiating factor for the unconventional shale gas formations are their adsorption capacity on surface areas associated with organic content and clay (Sondergeld 2010), as shown in figure 16 for a mud-rock sample on a scale of 500 nm .

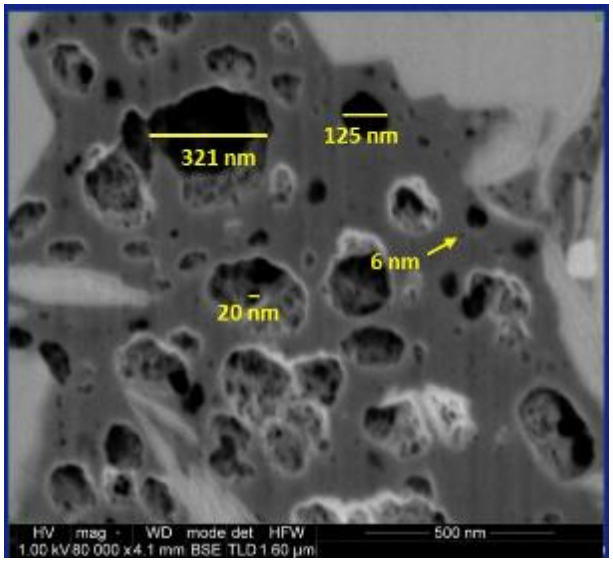

Figure 16 - BSE images of a region of kerogen having varying organic matter porosity in Shale samples (Curtis *et al* 2010).

The organic matter is mostly a combination of kerogen, bitumen and mobile hydrocarbons and is mostly reported as Total Organic Content (TOC). They highly impact the shale

properties by lowering the density, increasing the porosity, acting as a source of gas, imparting anisotropy, altering wettability and introducing adsorption. The kerogen, which is assumed to be a nano-porous organic material dispersed within in the inorganic matrix, in Barnett is mostly type II (tends to produce oil and gas), with a minor mixture of type III (only gas). Thermal maturity is also an important parameter used in the evaluation of oil and gas. Vitrinite reflectance (Ro) is commonly used as a thermal maturity indicator. Studies of the Barnett shale in the Fort Worth Basin show that highest gas rates occur at Ro > 1.4%.

In comparison with conventional gas reservoirs, shale gas may produce a considerable amount of gas through desorption (Mengal and Wattenberger, 2011), as can be seen in figure 14 (a). Adsorption at the gas-solid interface is commonly assumed to be the enrichment of one or more components at the interface layer (Sing *et al* 1985). The organic content in shale has a strong adsorption capacity due to large surface area and affinity to methane. And this must be incorporated in our simulation models for shale gas reservoirs. According to International Union of Pure and Applied Chemistry (IUPAC), six different types of adsorption mechanisms have been defined. The adsorption isotherm shape is closely related to the properties of the porosity system, the adsorbate and the solid adsorbent (Silin *et al* 2012).

The most commonly used adsorption model for shale gas is the Langmuir isotherm, which assumes that there exists a dynamic equilibrium at constant temperature and pressure in between adsorbed and non-adsorbed gas (Yu *et al* 2014). It assumes a single layer of

molecules covering the solid surface. It is to be noted that higher Langmuir pressure releases more gas at the same reservoir pressure, as can be observed from figure 17(b).

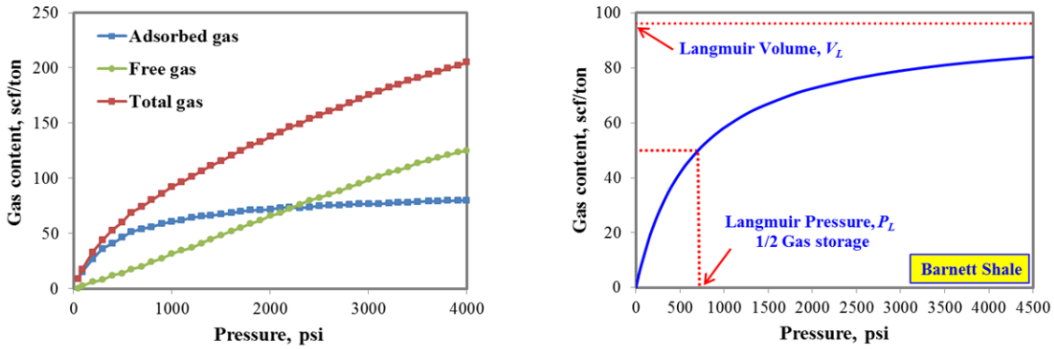

Figure 17 - a) Comparison of Gas content (Free + Desorbed) from a sample from Barnett. b) Langmuir isotherm curve for Barnett formation (Ye *et al* 2014).

3.2 Langmuir Volume and TOC

For most Shale reservoirs, the presence of mature organic matter is observed by an apparent increase in porosity logs (DlogR - Passey's Method). With maturation of kerogens to hydrocarbons, the resistivity increases and hence can be observed on resistivity logs. But we don't have any log data available for this well. Therefore, we would be taking a different approach to approximate TOC for this formation.

Tongwei *et al* (2012) proposed a regression based on empirical analysis that gave a relation between TOC and V_L for different shale reservoirs. This relation was obtained from various sorption isotherms in the temperature range of about 65 °C.

$$\mathbf{V_L = 1.34 * TOC + 0.0134} \quad (6)$$

Where V_L is in mmol(CH_4)/g of rock and TOC is in weight%.

It was observed that the maximum Langmuir CH_4 adsorption capacity is greatly affected by the TOC content (Lu *at al* 1995), as can be seen in figure 18 which shows a plot for this relationship.

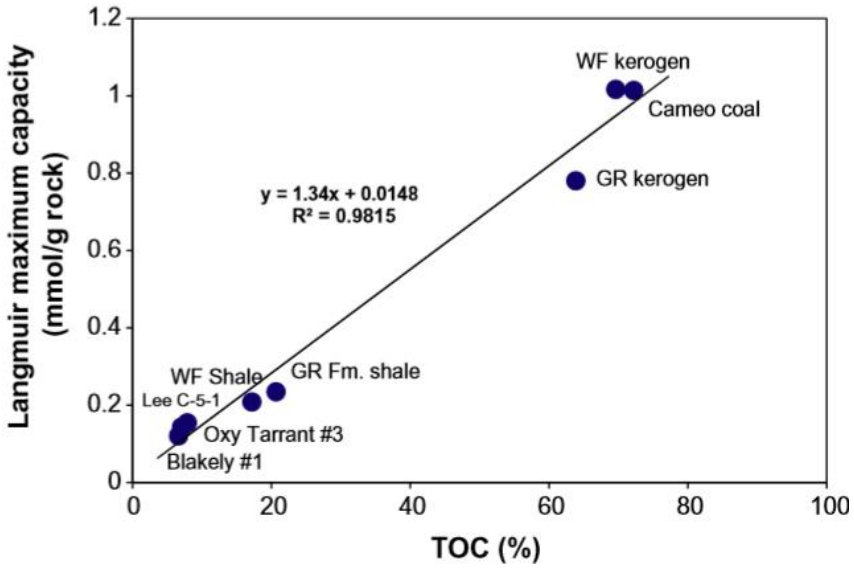

Figure 18: Linear Relation between Langmuir Volume and TOC in Shale plays around the world.

CMG IMEX takes input parameters of Langmuir volume, Langmuir pressure and intrinsic rock density for this purpose, which describe the desorption process. After modelling desorption in the matrix part, we would see that how much our results are impacted by

this process. We expect to see an increase in production because additional TOC would increase our Gas in Place. Desorption for the fracture part would be set to zero, as it occurs only in the organic rich shale part.

We would now run the model for 5 different TOC values of 1, 4, 7, 10 and 13 %., which was the observed range of TOC in Barnett formation, from literature. The Langmuir pressure for the matrix part is taken as 2020 psi (Tongwei etal 2012). The Langmuir volume for methane varies for these values, causing the Langmuir isotherm to significantly change. The Langmuir isotherm parameters that were used in the model are present in the table 2 below.

Table 2 - Adsorption parameters for each case considering desorption in Barnett shale model (assuming no diffusion)

Case	TOC	P_L (Psi)	V_L (scf/ton)	Rock Density (lbm/scf)
1	**1 %**	2020	19.06	167.5
2	**4 %**		47.6504	
3	**7 %**		75	
4	**10 %**		104.83	
5	**13 %**		133.42	

Figure 19 compares the cumulative gas production for the 5 different cases, where the simulation lasts for 7 years. The well is produced on AOF, using maximum surface gas rate of 1,500,000 scf just for the first day. It can be observed that in the initial period of the drainage process, there is very little difference among these cases because the process is supported by the free gas that exists in the pore system. Also, in the early time

production – the reservoir pressure is high and therefore the desorption contribution is insignificant. But as time proceeds, the effect of desorption from kerogens become more pronounced, as reservoir pressure depletes. As we increase the TOC values, the production increases. Using the case without desorption as the base case, the cumulative production for cases 1-5 increases by 2.83, 6.67, 10, 13.79 and 17.1 % respectively. Hence, neglecting desorption might lead to underestimating gas potentials, especially in shale formations with higher TOC values.

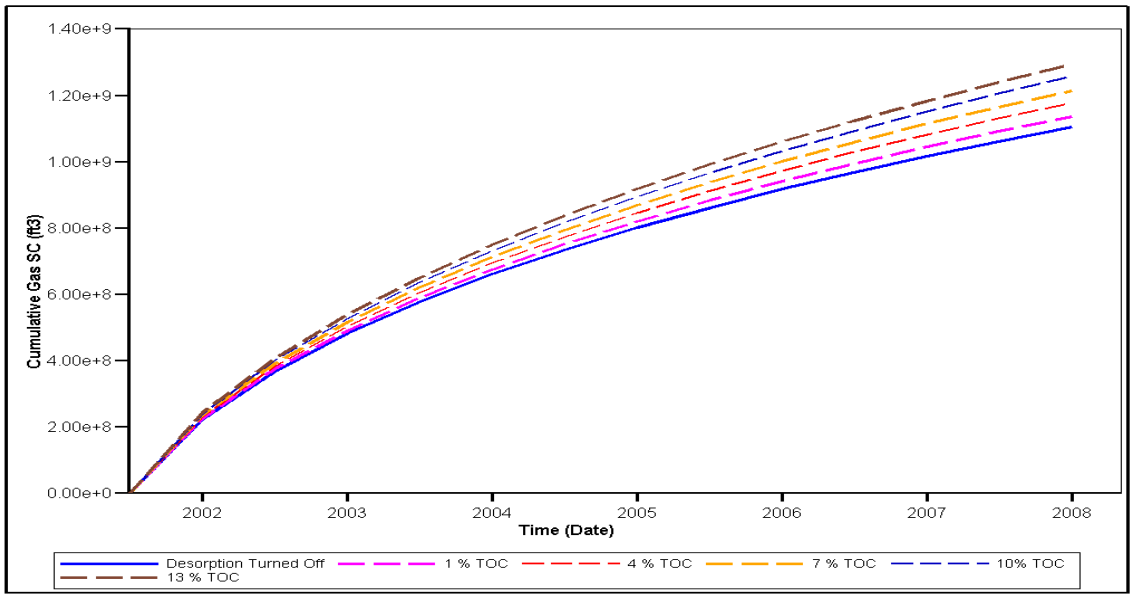

Figure 19 - Cumulative Gas Production for 5 different cases considering different values of TOC for desorption in our model.

Figure 20 presents the results for the average pressure for the 5 cases considering different values of TOC for desorption. The phenomenon of desorption helps to maintain the

pressure in the reservoir. This effect would become more prominent for higher Langmuir pressure values.

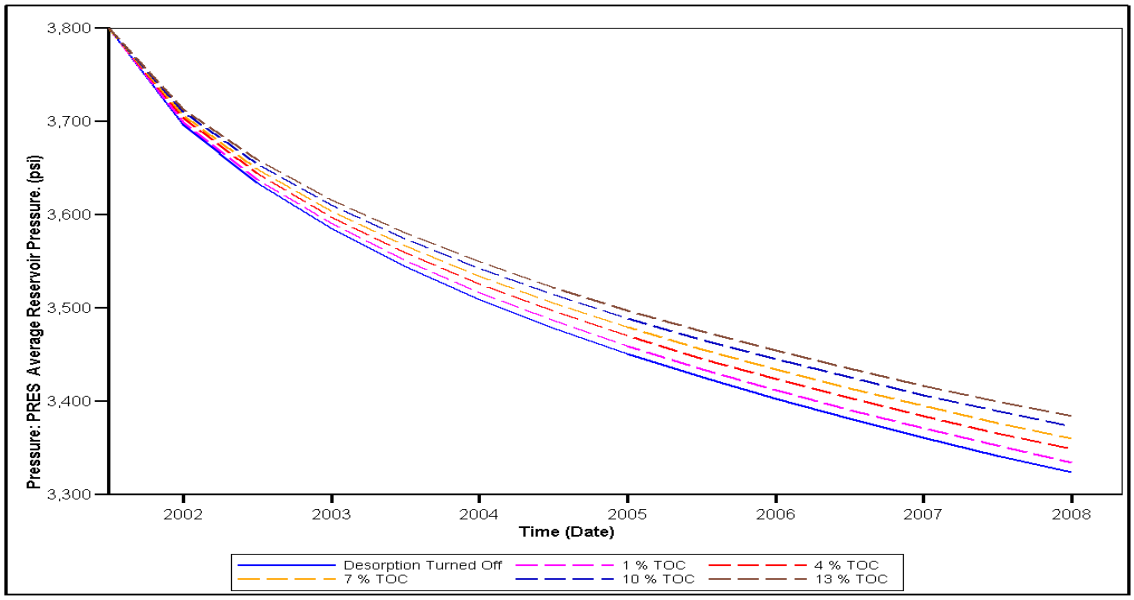

Figure 20 - Average Reservoir Pressure profile for 5 different cases considering different values of TOC for desorption in our model.

3.3 Forecast Prediction

Shown below (figure 21) are the results of the prediction runs, which was made for 30 years with desorption turned on. For the initial 8 years, we have an overlap of cumulative production because of the model being produced at constant rate constraint. But we see a clear difference in predicted average reservoir pressure profiles, with desorption helping to sustain the matrix pressure (by about 75 psi as compared to the case without desorption). Also, it seems to increase the cumulative gas production by about 11.6 %. The Langmuir

pressure used was 2020 psi, Langmuir volume was 0.0373255 Scf/lb for a rock density of 156 lb/scf (average density of Barnett Shale from Kathy etal 2011).

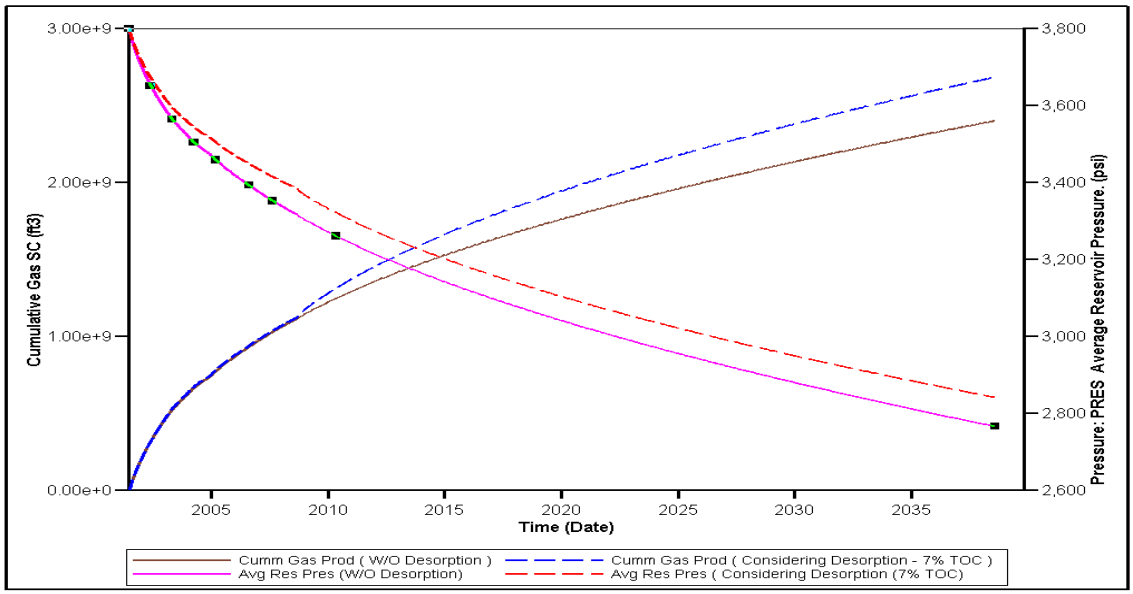

Figure 21 - Cumulative gas production and average reservoir pressure plots for runs made on our reservoir model considering diffusion. This was done on existing production constraints for the initial 8 year period, after which the run was for 30 years.

Since the well model was produced on gas rate constraint, we couldn't observe the effects of desorption for the first 8 year period. To tackle that, we switch the primary constraint to BHP and the surface gas rate is used as the secondary constraint instead (shown in figure 22 and 23). This caused the simulation time to increase from 3 minutes to 21 minutes for a single run, but helped reduce the uncertainty in parameters that might have existed for the vertical flow performance using tubing tables.

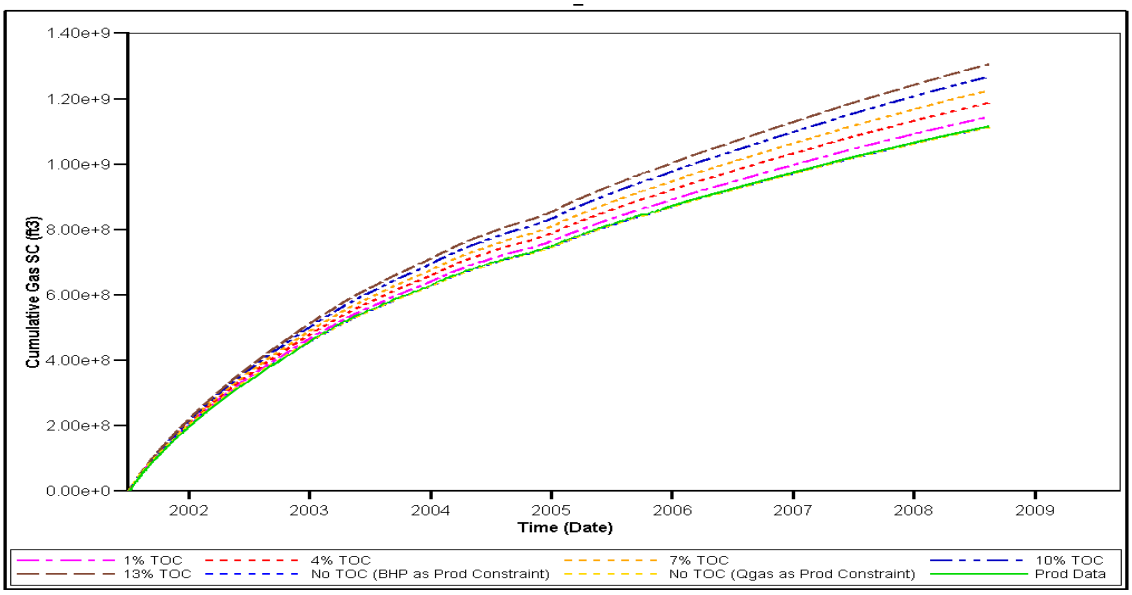

Figure 22 - Results for cumulative gas production over time. This run used BHP as the primary constraint (instead of gas rate) for cases considering various TOC values, against the base case that did not consider desorption.

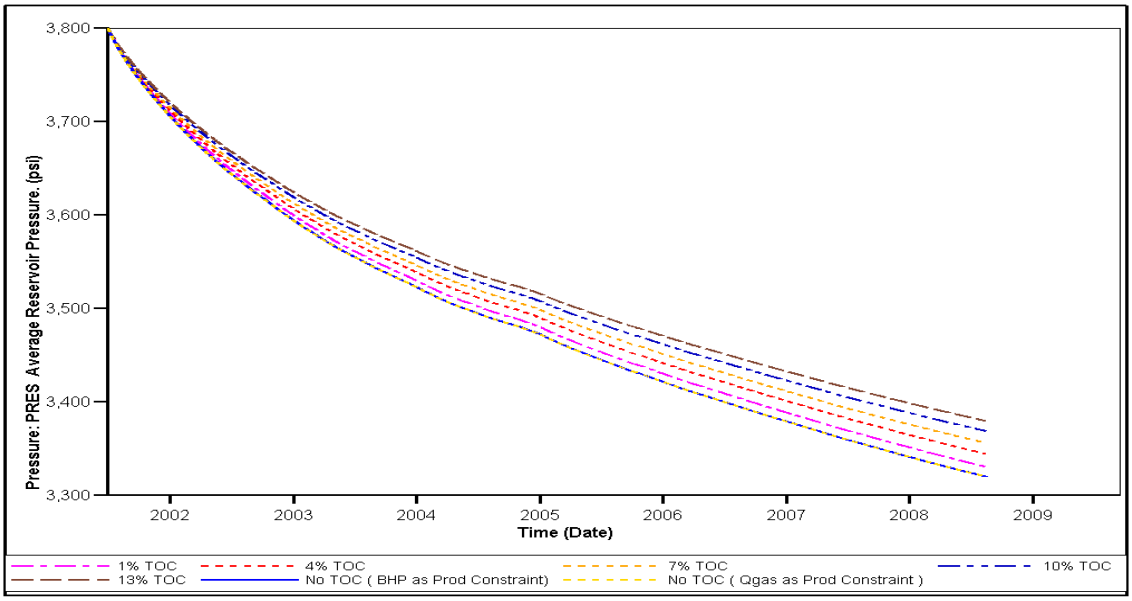

Figure 23 - Results for average reservoir pressure over time. This run used BHP as the primary constraint (instead of gas rate) for cases considering various TOC values, against the base case that did not consider desorption.

Results for cumulative gas production show that our estimates can increase by as much as 17% (for 13% TOC) if desorption process is modelled, for the same BHP constraints. The pressure stabilization effect is around 2% with 13% TOC, an increase of 60 psi after an 8 year period.

Thus, we can conclude that effects of desorption are dominant for higher TOC values and lower pressures. Additionally, it sends us the signal that some of our assumptions for the SRV region while doing the history match were not correct because this process would help to increase the production contribution from the shale matrix part.

3.4 Uncertainty Assessment for TOC using Monte Carlo Simulation

One of the major purpose of reservoir engineering is to estimate recoverable oil and gas volumes and predict production rates throughout the life of the reservoir. Prediction of production rates and cumulative production play an important role in decision making for Exploration Play Assessment, Development Drilling Locations, Risk and budgeting of potential E&P developments and corporate reserves evaluation.

In the previous section, we created deterministic production forecast. But it has now become an industry practice to generate a spectrum of realizations for the forecast using multiple simulator runs. Monte Carlo simulation is used to deal with the uncertainty with input parameters used for the reserves in place volumetric calculation. Instead of a single value (deterministic approach), it allows us to provide a range of values for water saturation, porosity, areal extent and recovery factors.

We run two cases for this cases – around 8000 iterations were run using a proxy equation, along with equal number of runs for simulator. Results from both the approaches showed similar results, as shown in table 3.

The Total Organic Content by weight % for Barnett shale is reported as average values of 3.16-3.26 by Jarvie (2004) , 3.3-4.5 by Montgomery *et al* (2005) and 2.4-5.1 by Jarvie *et al* (2007). Additionally, we plotted TOC values (from literature) for around 75 wells producing from the Barnett formation, and found the distribution to be normal. Hence, we use the normal distribution to describe it, with a mean of 4.5 and standard deviation of 1.16. Tails were clipped off, so that they do not extend to infinity. The distribution used is graphically shown in figure 24.

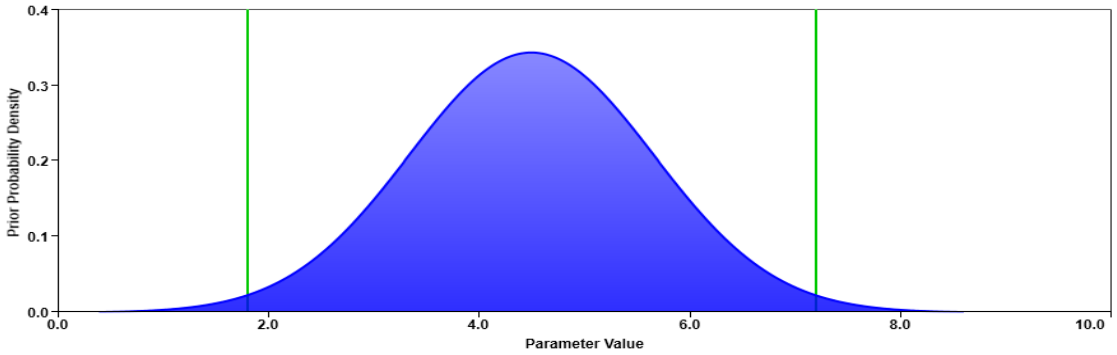

Figure 24 - Normal Distribution (4.5, 1.16) describing TOC range for the Monte Carlo Simulation.

Reserve estimates are extracted from a Monte Carlo simulation at confidence levels of P90, P50 and P10. Results are shown in table 3.

Table 3 - Results obtained from the Monte Carlo Simulations taking TOC as the varying parameter and studying the range of output parameters like cumulative gas production and average reservoir pressure.

Model for Monte Carlo Simulation	# of Experiments	Output Parameter	Mean	P10	P50	P90	Max Value	Min Value
Proxy Model	8000 (iterations)	**Pressure (psi)**	3351.79	3344.68	3351.37	3357.74	3380.5	3315.5
		Cumulative Production (scf)	1.18725 E9	1.16479 E9	1.18565 E9	1.20574 E9	1.283 E9	1.11555 E9
Reservoir Simulator	8000 (runs)	**Pressure (psi)**	3351.25	3344.69	3351.37	3357.73	3378.	3325
		Cumulative Production (scf)	1.1853 E9	1.16498 E9	1.18565 E9	1.20573 E9	1.272E9	1.1155 E+9

If we observe the cross-plot of cumulative production with TOC values as shown in figure 25, we see an increasing trend which shows that both the parameters are directly proportional to each other. But 1% increase in TOC causes our production to increase by just 1.6% (1.8 E+7 scf). If we assume current gas prices of 2.82 USD/MMBtu, that would amount to an additional profit of just 50760$ in 8 years. Thus, we should have sufficiently large TOC values for our formations to see their impact on the economic decision making analysis.

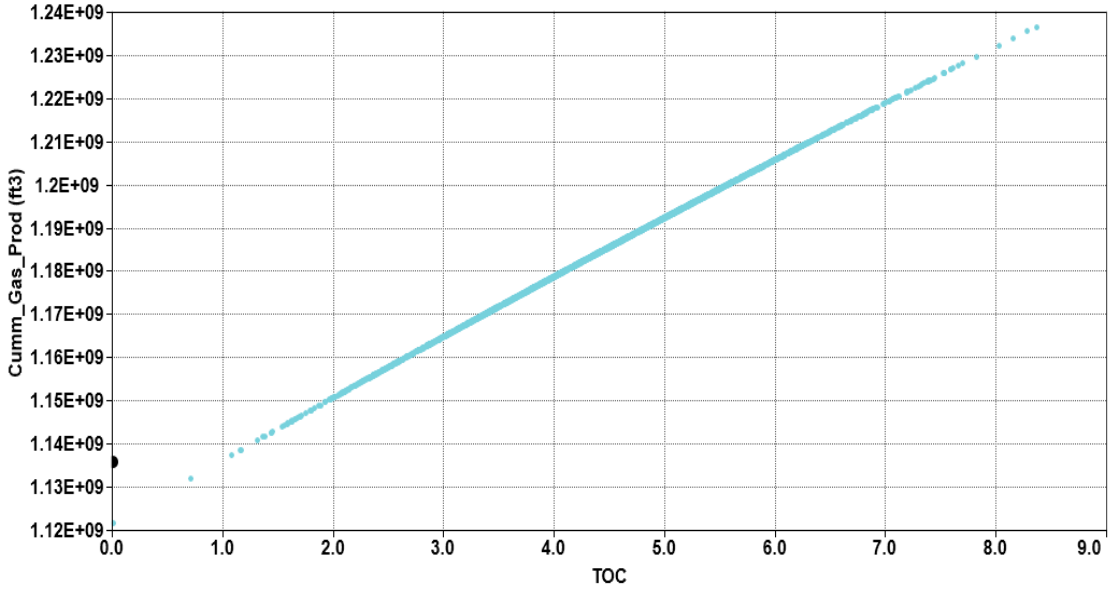

Figure 25 - Cross plot of cumulative production against TOC obtained from the results of simulation runs done for Monte Carlo Simulation.

The results, plotted as CDF and PDF histograms. after 8000 simulation runs for cummulative gas production and average reservoir pressure are shown in figure 26 and 27. It can be seen that the resulting distributions are normal too, which validates our point that cummulative rate increase our gas production and helps in a bit of pressure stabilization. The mean of the resulting distribution for production forecast is 1.18526E+09 scf,. The P10, P50 and P90 values are 1.15472E+09 scf, 1.18552E+09 scf and 1.21516E+9 scf. respectively. Hence, the gas production is increased by 8.5%, for cases lying in the P90 region, if we consider desorption.

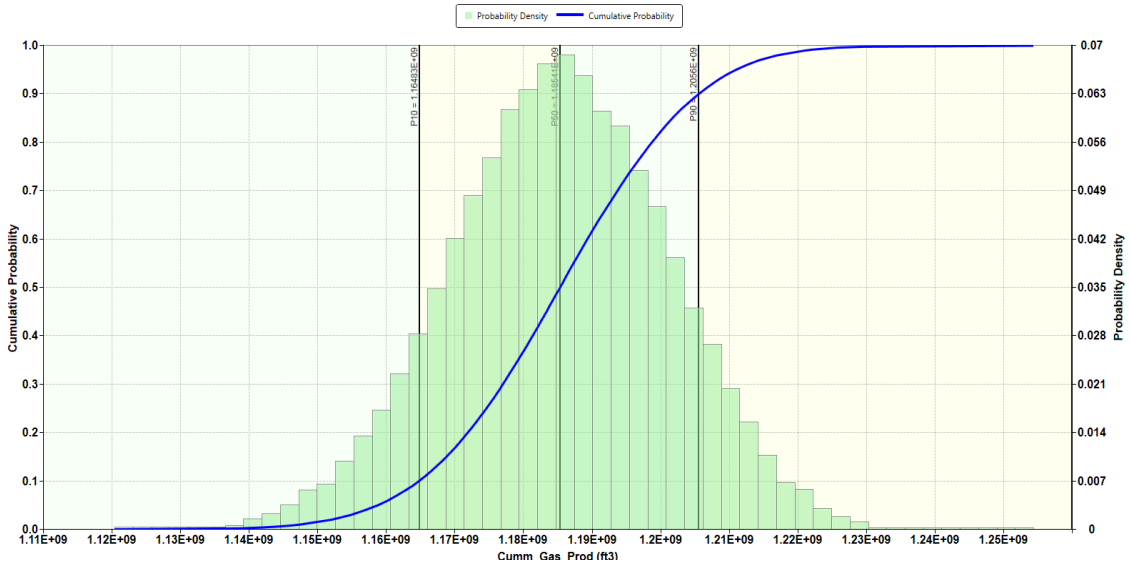

Figure 26 - Monte Carlo Results for Cumulative Gas Production, after assuming desorption in model.

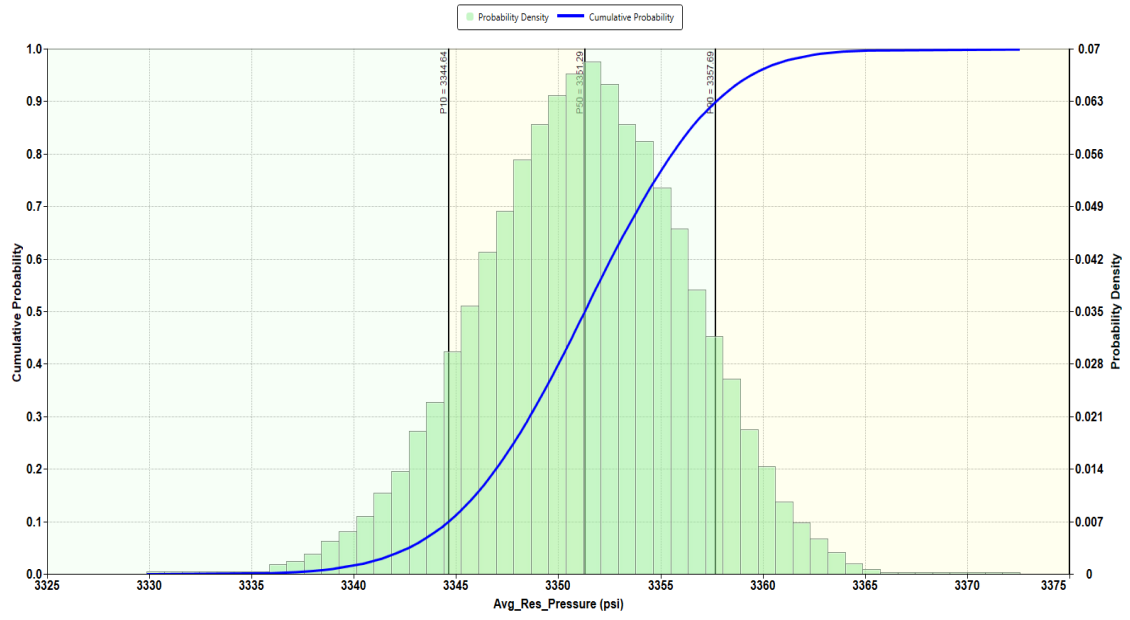

Figure 27 - Results from Monte Carlo Simulation for Average Reservoir Pressured after assuming desorption in our model.

The mean of the resulting distribution for average reservoir pressure is 3351.2 psi. The P10, P50 and P90 values are 3344 psi, 3351 psi and 3357 psi respectively. Hence, it is not affected significantly by increasing TOC values.

3.5 Conclusions

After setting up our reservoir model, we studied the effects of desorption mechanism on gas flow. Desorption contributes to around 40% for our gas in place. But Barnett Shale fails to produce all of it because of very low permeability. We link up the production from nano-porous organic matter in the matrix using Lanmguir volume and TOC, and show how our cumulative production increases with increasing TOC.

The desorption process is mainly dominant in the later period of production, when the free gas has been produced from the bigger pores of the inorganic matrix part causing bigger pressure drops. Hence, it has minimal effect on the initial well productivity.

CHAPTER IV
EFFECTS OF DIFFUSION

As discussed before, the shale gas strata ranges from few micrometers to nanometers. Their small size and large pore density makes the exposed surface area quite large. Therefore, despite small molecular diffusion – the flux distribution could be important. One of the issues that needs to be investigated is the impact of diffusion within the kerogen part and its effect on gas production.

4.1 Dynamic Apparent Permeability

In chapter I, a parameter called apparent dynamic permeability was defined, which was calculated in the micro scale model as a function of matrix pressure (Yan *et al* 2013), and is represented by equation (5). This concept comes from the fact that apparent permeability deviates from the Darcy permeability because flow in low permeability reservoirs occurs by various other phenomenon than the viscous flow regime represented by Darcy's law (Civan *et al* 2011). Flow undergoes a transition into molecular flow regimes for shale reservoirs that have pore size below the range of 10 nm (Andrade *et al* 2011).

The apparent permeability correction, as computed by Yan *et al* (2013), can be conveniently incorporated into our numerical simulation model as a pressure-dependent permeability function using rock tables.

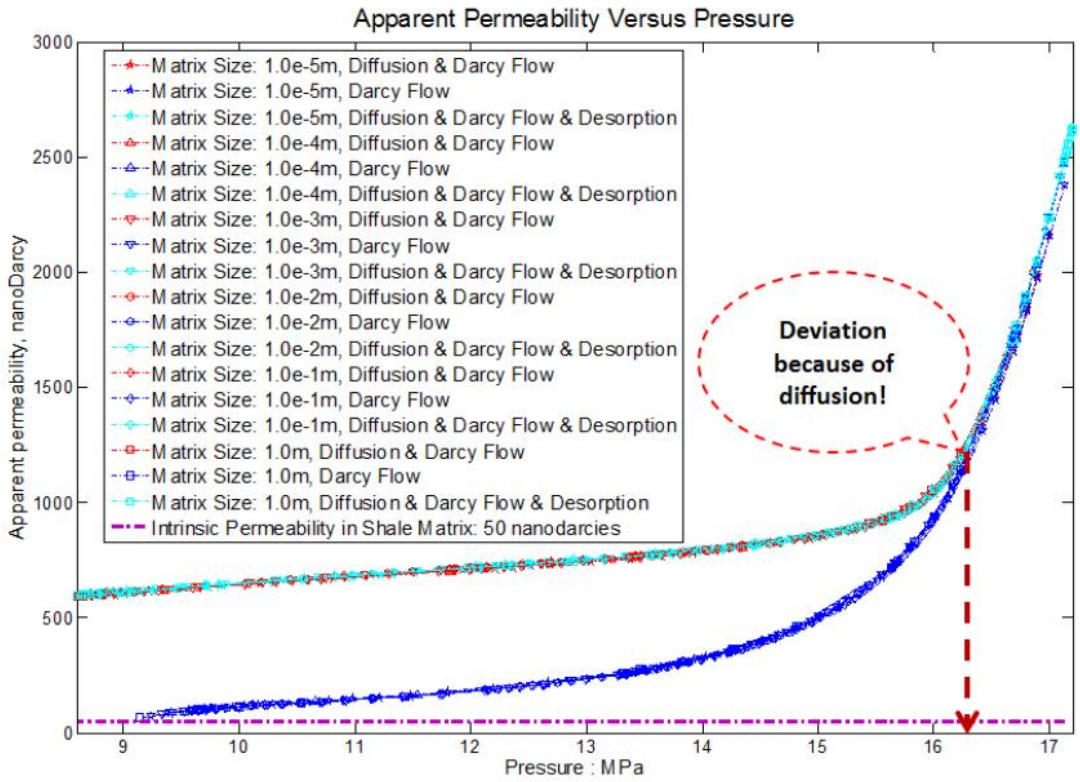

Figure 28 - Apparent Permeability as a function of pressure, as proposed by Yan *et al* (2013) to upscale assumption of micro scale model to a reservoir scale.

The *findings from his model simulations* showed that the apparent permeability is independent of matrix and fracture size, and is hardly impacted by the desorption process. This is shown in figure 28 and 29. Its main differentiating factor from the Darcy permeability was the effect of diffusion that causes deviation. Early time period for both the permeability's overlap, because of the dominance of Darcy flow causes free gas in larger pores to flow into fracture system. This deviation is in agreement with results found by Javadpour *et al* (2009), where he considered Knudsen diffusion and slip flow, along with advective gas flow in nano-pores.

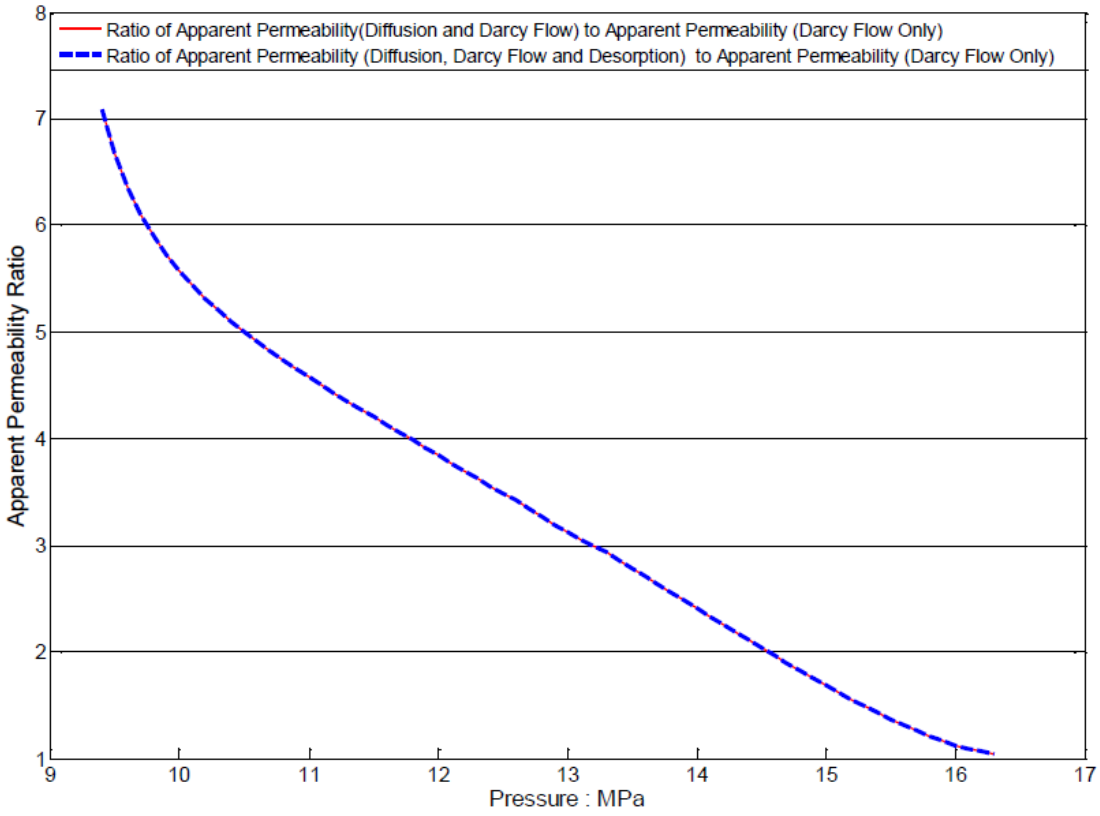

Figure 29 - Apparent Permeability Ratio, shown as a function of matrix pressure, takes cares of modelling diffusion and the transient affect between matrix and fractures in Shale.

4.2 Results comparing Different Flow Mechanism

To better evaluate the diffusion process, desorption is turned off in the model. Our assumption is that diffusion is the only mechanism causing gas flow from the nano-pores of the kerogen part, and works along with Darcy flow for the micro pores that exist there. If we don't model diffusion – we wouldn't be able to produce the gas in the extensive

nano pore system, where Darcy law is not applicable because of small pore radii. This would result in a much lower reservoir pressure drop production commences.

To capture the dynamic permeability effect, modifications are made in the rock compaction table for matrix part that causes permeability to act as a pressure dependent function. This is an effective way to capture molecular affects under Fickian diffusion and causes the permeability to increase at lower pressures. Point to be noted here is that it is not related to stress dependence of the rock matrix.

Figure 30 and 31 show the relationship of cumulative gas rate and average reservoir pressure with time. If we compare the ultimate cumulative production of cases considering diffusion to our base case in figure 30, we see an increase of around 25% which is much greater in magnitude as compared to the results we obtained for desorption for high TOC values. Also, it seems to accelerate the pressure depletion process, in contrast to the stabilization affect by desorption as seen in figure 31. Thus, we can easily conclude that diffusion greatly helps in draining gas to the well bore, at a later time of production when free gas from larger pores has been produced.

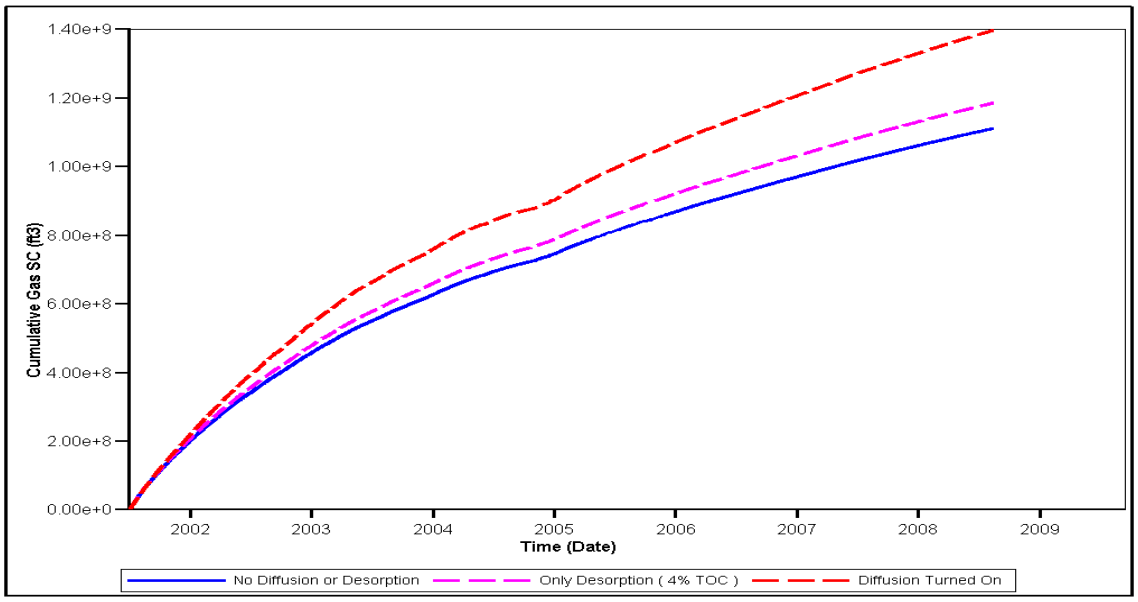

Figure 30 - Effects of Diffusion on cumulative gas production, compared against results from base model assuming with and without desorption.

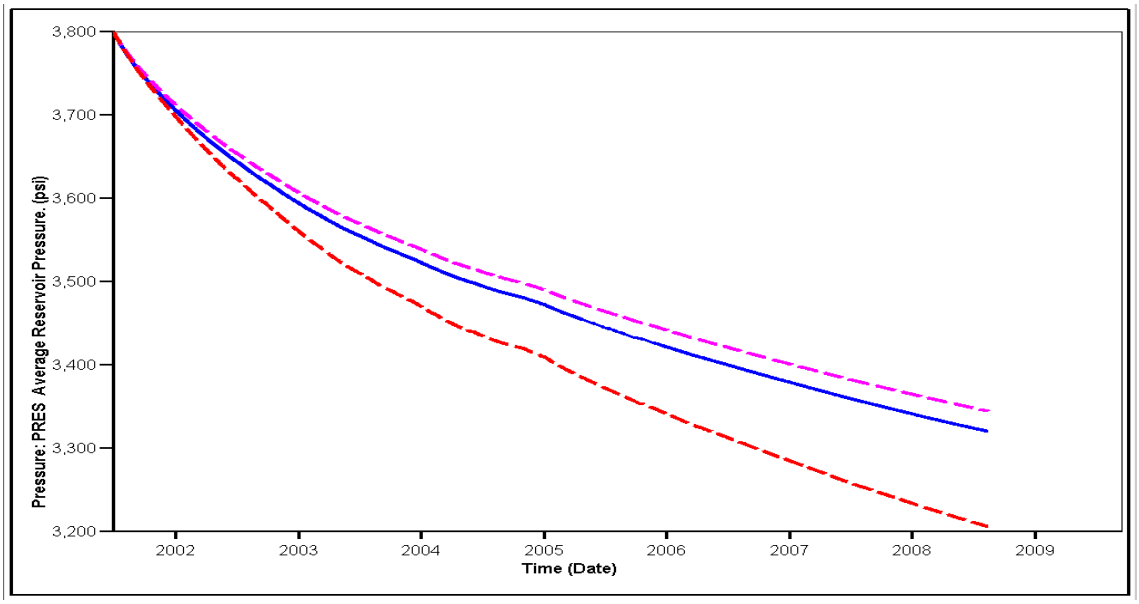

Figure 31 - Effects of Diffusion on average reservoir pressure, compared against results from base model assuming with and without desorption.

We finally turn on both diffusion and desorption and compare the case against our initial runs and cases considering diffusion and desorption separately. As observed from the results shown in figure 32, the production has increased by 37% on constant BHP constraints for production. The average reservoir pressure seems to be in between the results obtained by considering diffusion and diffusion and desorption occurring simultaneously. It is because of the fact that desorption helped to maintain the pressure, while diffusion kept it low because of gas drainage from nano-pores.

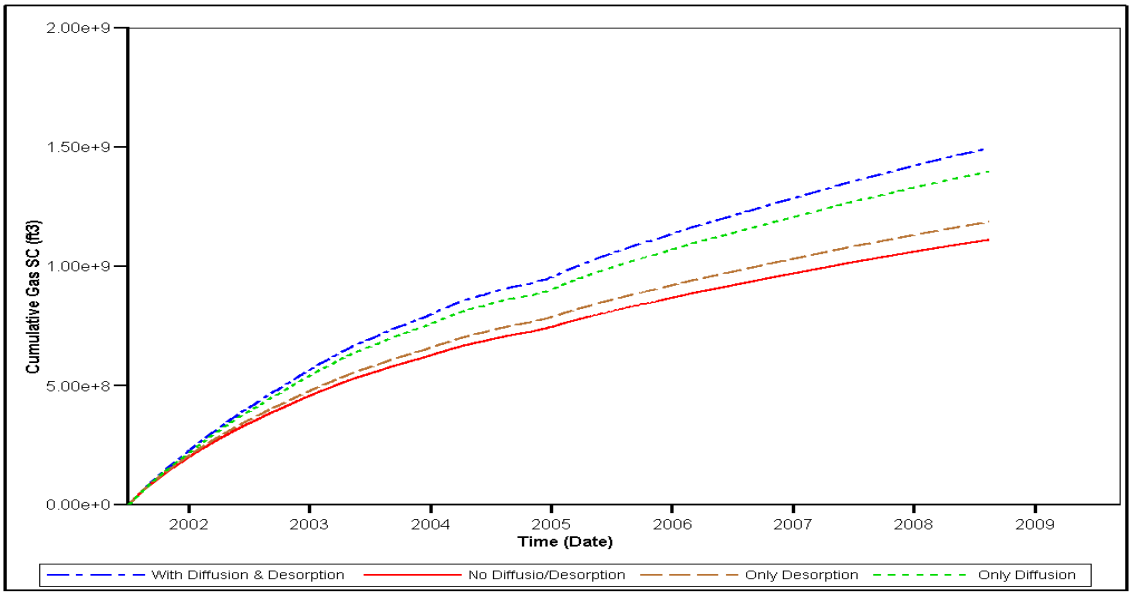

Figure 32 - Cumulative gas rate curves comparing effects of different mechanisms against the base model assuming only Darcy flow

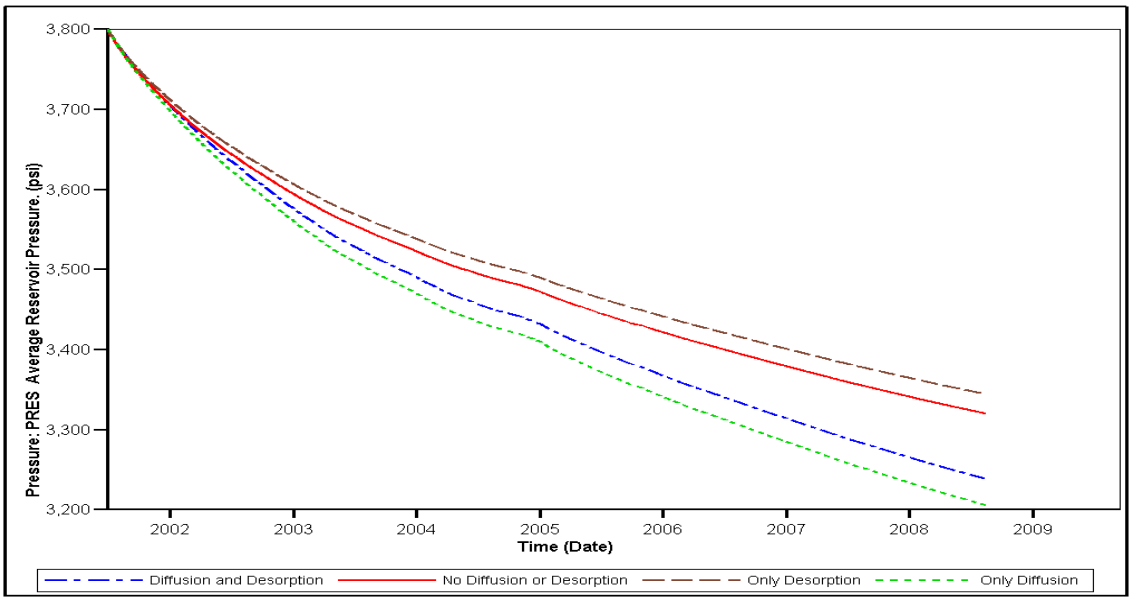

Figure 33 - Average reservoir pressure curves comparing effects of different mechanisms against the base model assuming only Darcy flow

We now present the saturation and pressure profiles for the cases considering diffusion and desorption compared to our initial case, in figure 34 and 35, with the well being produced for 8 years at BHP constraint. Red is the initial reservoir pressure while dark blue is the flowing bottom-hole pressure. We see that the sub micro Darcy matrix had drained not very far from the fracture network. It is quite evident that with additional mechanisms at work in addition to Darcy law, more gas is produced from the micro-pores in kerogen part and the nano pores with in the organic structure. It can be observed that more gas being fed by the matrix into the fracture system. We also see lower pressure contours resulting from drawdown around the wellbore region for the dynamic permeability case.

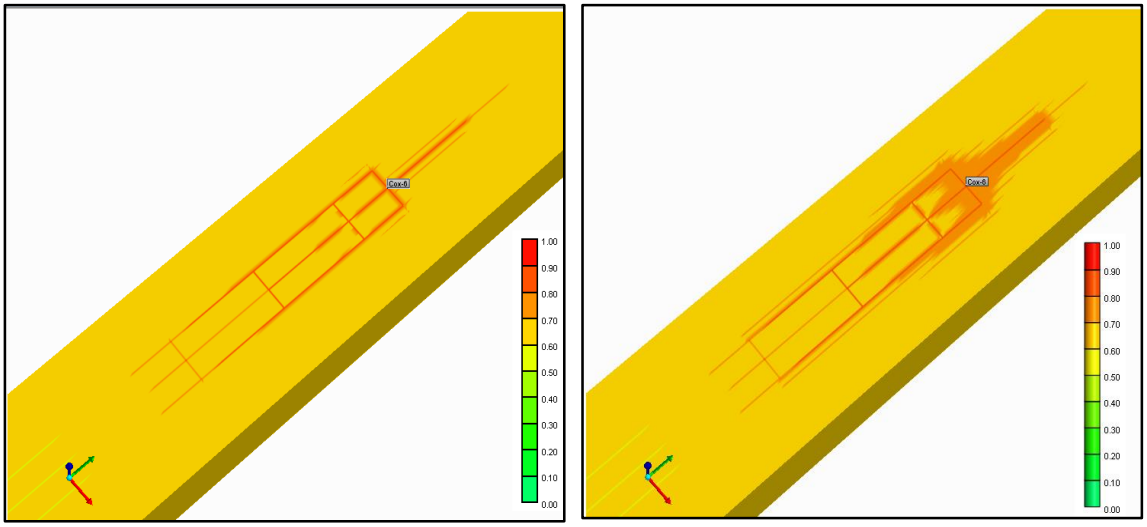

Figure 34 - Gas Saturation around fracture region shown on a 3D view of our reservoir model after 8 years of simulation. The first case is modelled without considering Diffusion and Desorption, while the second case takes those mechanisms into consideration.

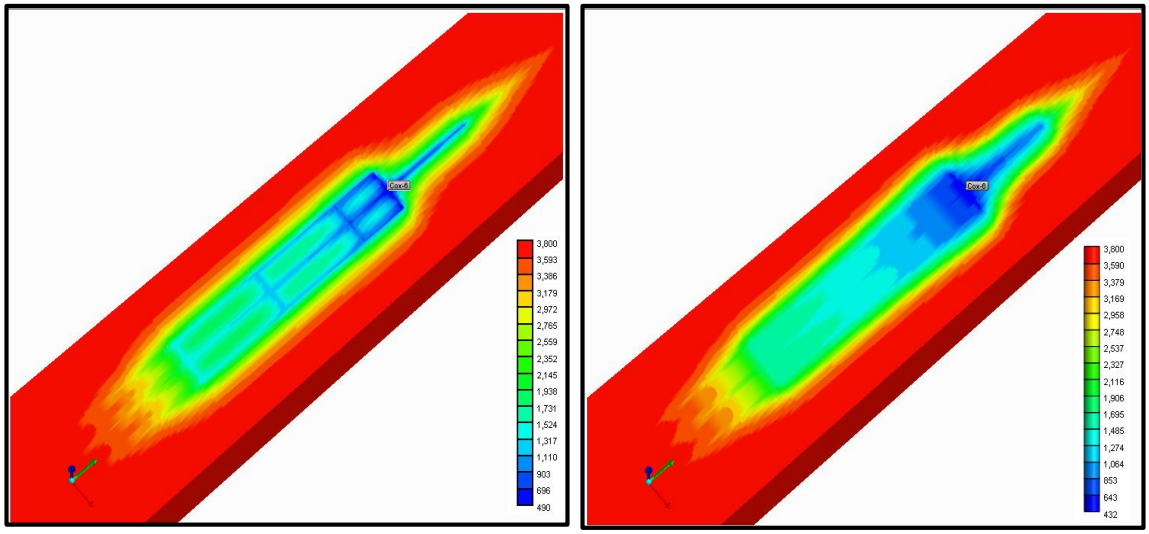

Figure 35 - Pressure profiles around fracture region shown on a 3D view of our reservoir model after 8 years of simulation. The first case is modelled without considering Diffusion and Desorption, while the second case takes those mechanisms into consideration.

One of our options could have been to simply switch on the molecular diffusion option in the numerical simulators that we are currently using. But our approach to model it is using the idea given by Yan *et al* (2013), which gives results that are in agreement with experimental observations for concepts like Knudsen diffusion, slip flow and advection. Also, since he modelled flow through nano and micro-pores by taking it to the micro-scale level - all the relevant physics come into play.

4.3 Conclusions

We have now up-scaled the assumption for flow in porous media of shale reservoirs. Results showed that Diffusion, whose main driving force is the concentration gradient, plays a dominant role in the low permeability matrix, increasing total gas transport capacity in pores. Also, the increased drop in pressure accelerates the gas drainage capacity towards the wellbore. When it is combined with desorption, our cumulative gas production increases by around 30%, which can help in explaining the high production trends from shale reservoirs that conventional models were in capable of predicting.

CHAPTER V

STUDYING IMPACT ON THE SRV VOLUME AND PRODUCTION FORECASTING

Before performing the history match, let us recall how the model has now been developed in agreement to the assumptions and objectives for modelling gas flow in organic, inorganic and fracture system of the shale matrix. During production, Gas is first produced from the fracture network driven by the Darcy law. Then gas is released from the inorganic material to the fracture system, because of concentration gradient triggered diffusion and pressure gradient triggered Darcy flow. Lastly, gas is fed from nano pores in the organic part to bigger pores of inorganic system resulting from diffusion only. The resulting pressure drop induces gas molecules to desorb from the kerogen surface.

The SRV region, its volume and properties, would now be studied after history match to see if it is affected by these flow mechanisms that cause a greater contribution of matrix towards production. Also, the resulting production forecast would be compared.

5.1 Sensitivity Analysis

The updated reservoir model is now used for sensitivity analysis of basic petro-physical inputs, like matrix porosity and TOC values, and properties related to our SRV, like natural fracture length, permeability and porosity, to identify which parameters have the maximum effect on our output. These would later be used to define the objective function,

used later for the history match error. Sensitivity analysis uses a limited number of simulation runs to determine the parameters that should be varied in subsequent studies and over what range. This information would help to design our history matching job, which requires a greater number of simulation runs.

Hydraulic fracture half-length and their spacing are not considered as tuning parameters, because we had data about them from micro-seismic survey and it would help us in achieving a unique solution. All this work is done using the CMOST module of CMG. Tornado plots for sensitivity analysis are shown in figure 36, for well head pressure.

Hydraulic fracture permeability was found to be the most sensitive tuning parameters for well head pressure. This is reasonable considering the fact that fractures permeability cause the gas to flow from low permeability shale matrix to the wellbore. Matrix porosity was another observed parameter that had an influence, because of the way it controls the OGIP and hence affects cumulative gas produced. One interesting find was that Langmuir pressure has a big impact on our Well head pressure, which can be explained by the higher amount of adsorbed gas release at higher pressures.

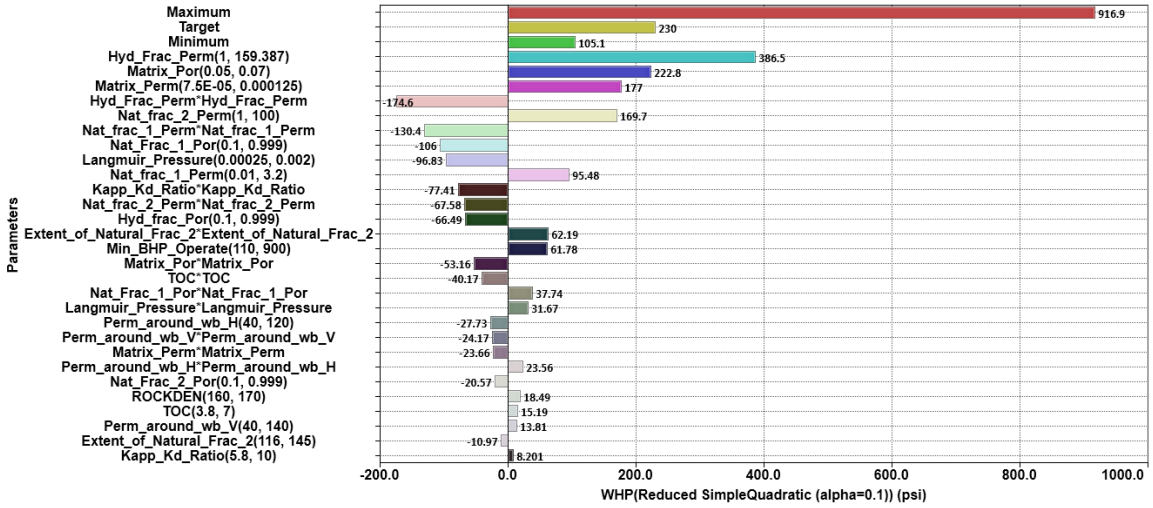

Figure 36- Tornado plot showing sensitivity analysis results of different reservoir parameters affecting the Well Head Pressure

5.2 History Matching

Before starting with the process, simulation results of the updated model considering diffusion and desorption were analyzed to identify major directions to improve this history match. They are shown in figure 37.

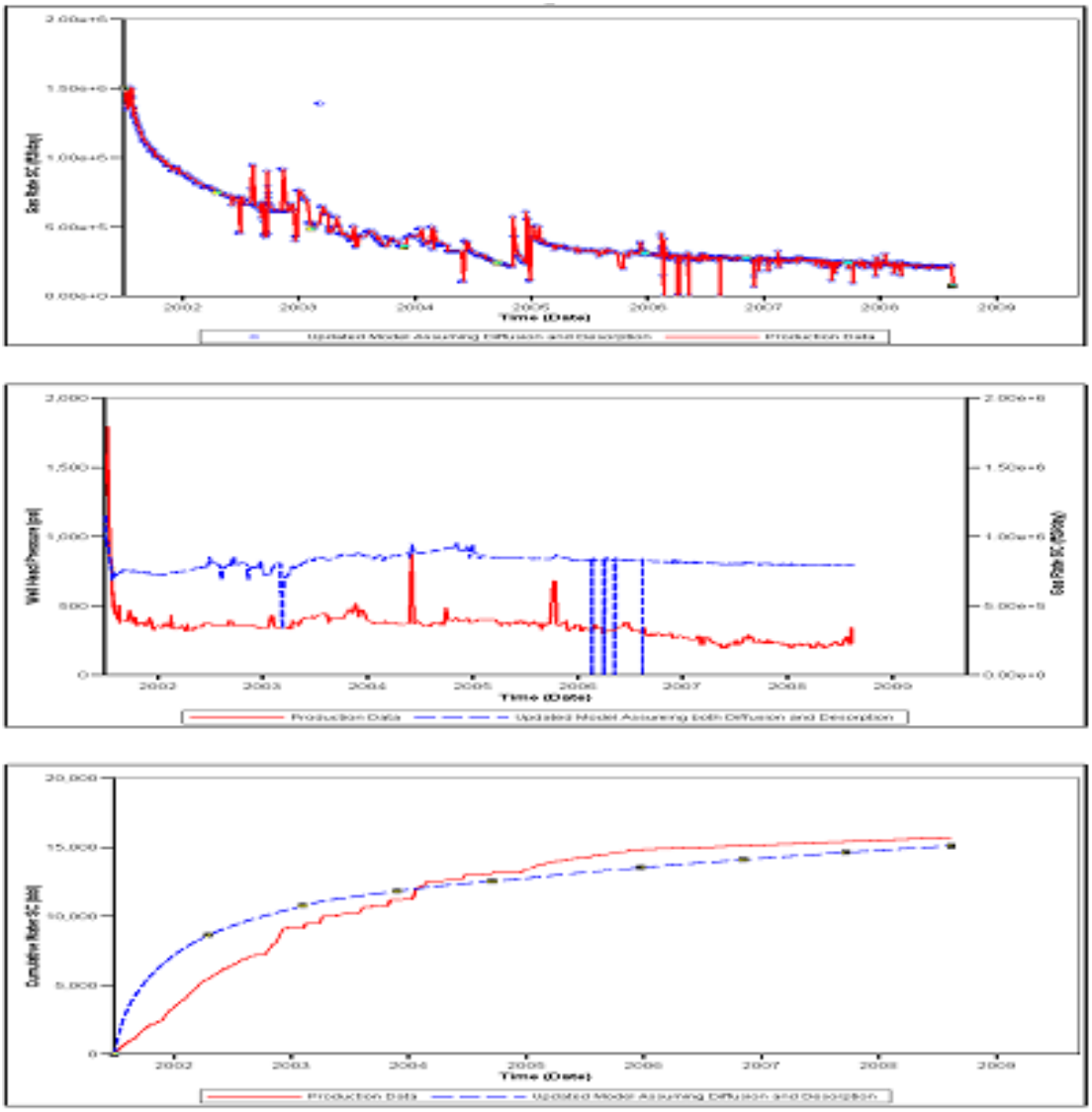

Figure 37 - Comparison of production data against model for cumulative gas, well head pressure and cumulative water production, prior to history match.

The areas that needs to be improved is to match well head pressure and to improve on the water production. Once the WHP is matched, the gas rates would match automatically because the model is constrained to gas rate. An objective function is developed for the well, which measures the relative difference between the measured and simulated results.

CMG DECE optimizer is used as the engine for this purpose. It can be described as an iterative optimization process that first applies a designed exploration stage and then a controlled evolution stage. The measurement error and weights used in objective function are shown in table 4 below.

Table 4 - Measurement error and weight assigned to historical production data, to be used in the objective function for history match.

Property	**Absolute Measurement Error**	**Weight**
Cumulative Gas SC	0	3
Well Head Pressure	0	1.9
Cumulative Water SC	500	0.35

Gas Rate is not used in constructing history matching error type objective function because it is a discontinuous step functions. This means that the rate value is not well defined at the boundary of each interval and could cause inaccurate calculation of the history matching error. The cumulative gas is continuous in time, hence it is used as a replacement for rates in history match error calculations. If the entire curve of a cumulative quantity is matched perfectly, it guarantees the corresponding rate curve will be matched as well.

The behavior of our model can be influenced a large number of reservoir properties. Therefore, the parameters are restricted to a set that would be most likely significant on our results based on our observations from the sensitivity analysis. Numerical simulation history matching process can be non-unique in shale gas reservoirs because of the complex

fracture network. However, the tolerance level for modelling can be constrained when estimates of permeability are available from core data and micro seismic data helps in determining the SRV and mapping the fracture network developed. This helps in obtaining a unique solution for the fracture conductivity (Mayerhofer *et al* 2010).

Fracture permeability, matrix porosity and permeability, permeability around the wellbore region, TOC, extent of the fracture system in SRV and minimum BHP for operating conditions are set as the parameters for history match. Matrix permeability, which can be a dominating factor for flow, is allowed to vary from 75-125 nano-Darcy. The tolerance limit for porosity is kept at +/- 2% + actual porosity of the model. This tolerance limit is normally acceptable because different laboratory procedures for the same core sample give porosities that lie in the same range as mentioned above (Wu *et al* 2013). This range depends upon different factors including whether the sample was crushed, sieved or taken as a core sample during the tests. TOC values are described as a normal distribution (mean = 4.5, S.D =1,24) which describes the range that has been normally observed in Barnett. 500 runs were made in automated history matching, which provided us with the best match (job # 202) – having a history match error of 2.9%. Figure 38-40 show that the match quality has improved considerably.

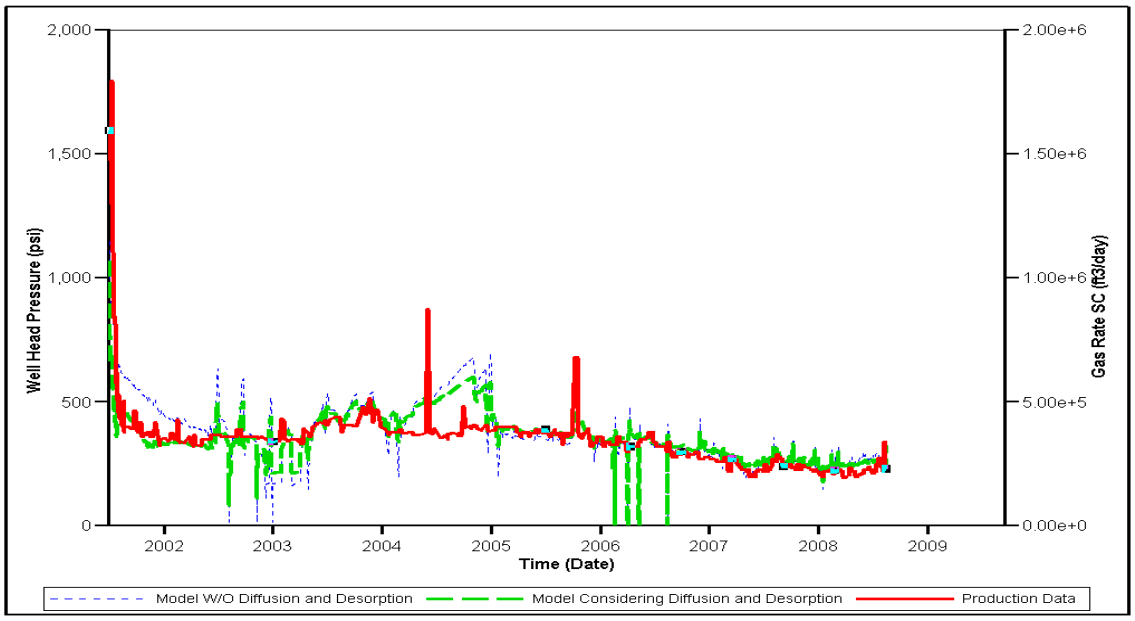

Figure 38 - History Match shown of the updated model for WHP, against production data and results from model that did not consider diffusion and desorption

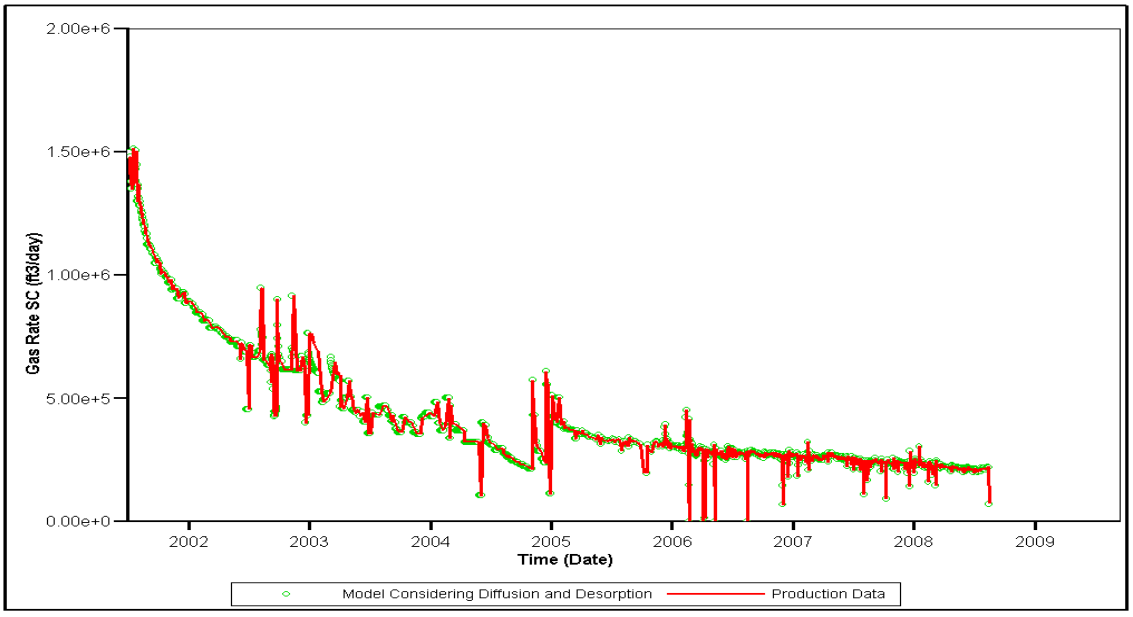

Figure 39- History Match shown of the updated model for gas rates, against production data and results from model that did not consider diffusion and desorption

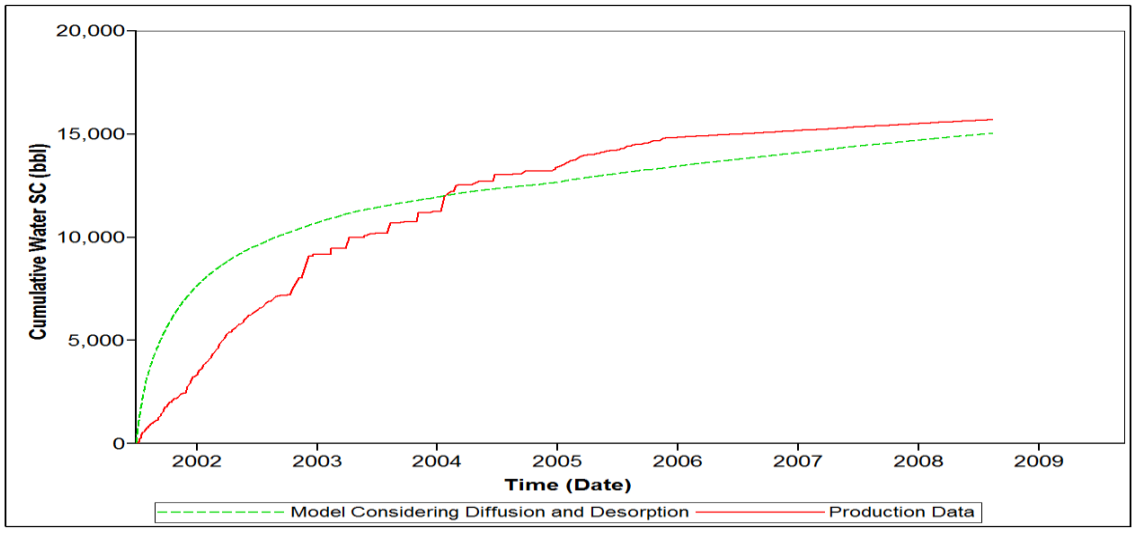

Figure 40 - History Match shown of the updated model against production data and results from model that did not consider diffusion and desorption

After the history match, the values of parameters related to SRV show a relative change in magnitude. This was intuitive, because of the improved recovery of gas from the organic porosity system. The SRV volume for the well was also changed. We saw the length of the natural fractures extending in the North-East and South-West directions get reduced by 16% and 9% respectively, which is marked in figure 41. The total extent of the fracture network is now reduced from 3000 ft to 2660 ft. Thus, this information can help us to improve completion design and well spacing, in field development.

Observing gas saturation profile for case considering diffusion and desorption, in figure 41, makes us realize that the gas drainage capacity has improved significantly in the matrix part. Pressure profile after 8 years of production shower lower drawdown pressures around the wellbore, resulting in greater production. This causes all the free gas to be produced

from larger pores and initiates the diffusion process from for flow from organic to inorganic part.

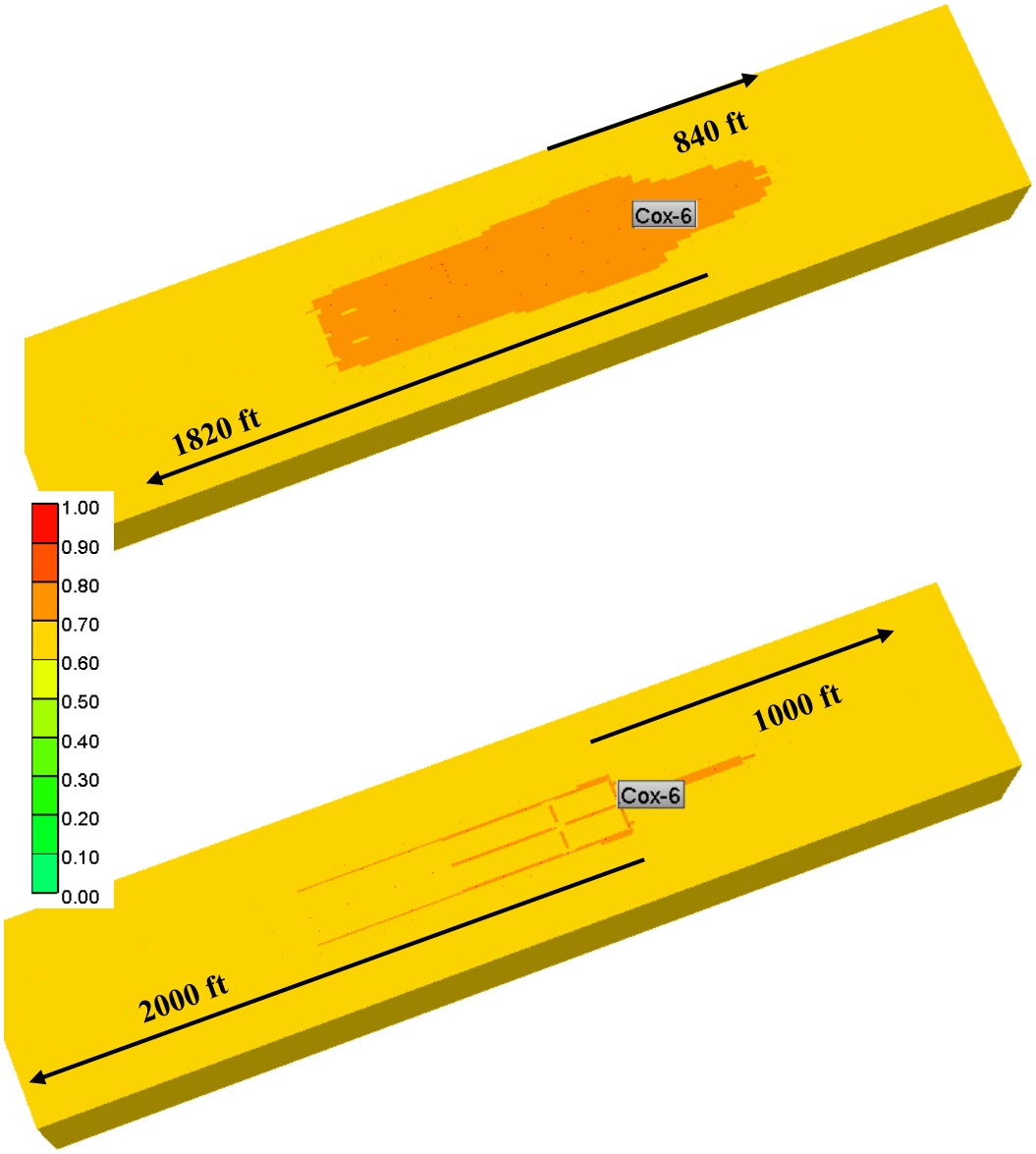

Figure 41 - Comparison of Pressure profiles around the wellbore drawdown region for updated model (considering Diffusion and Desorption) against base model. Changed volume of SRV is also marked on the model.

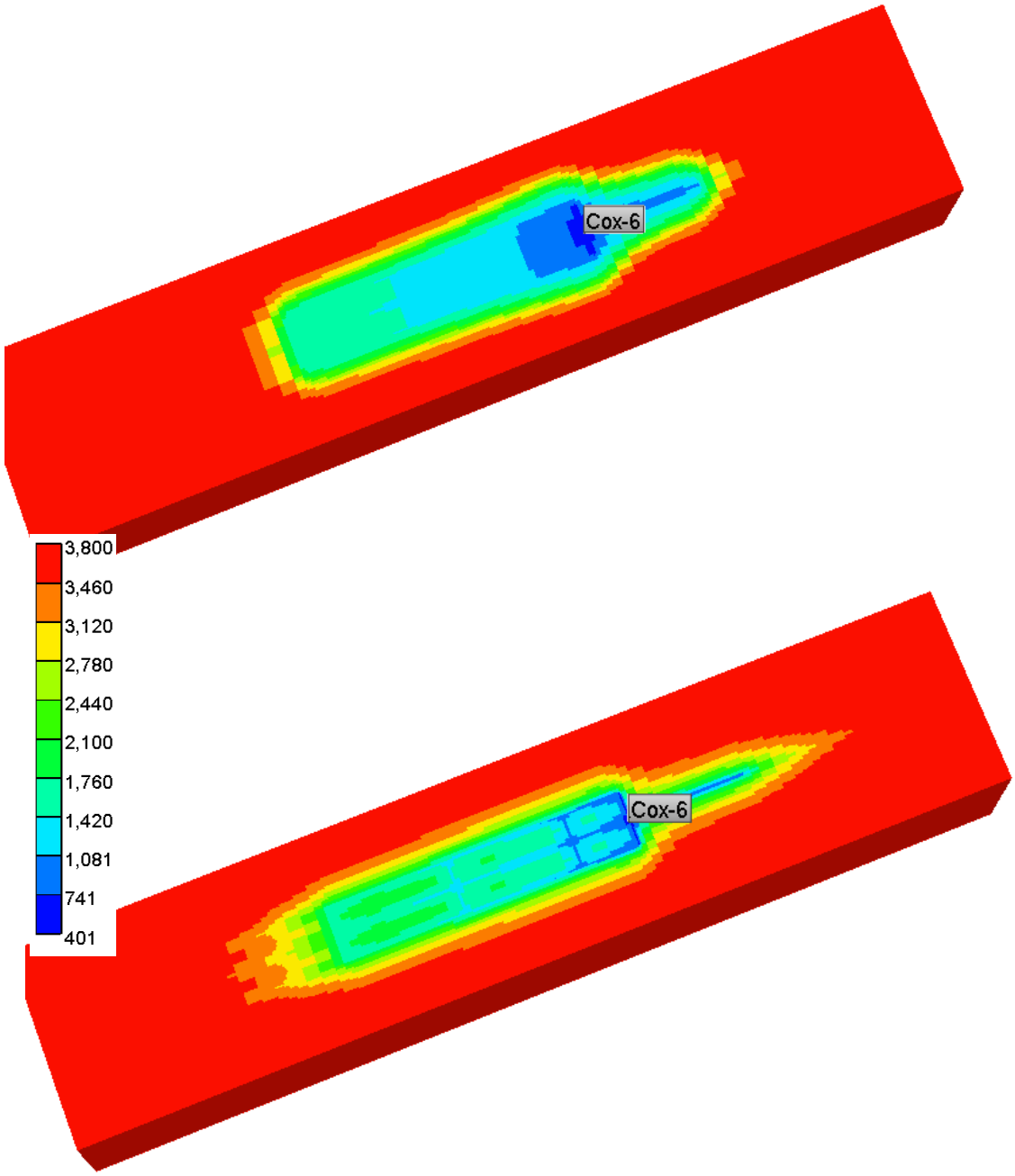

Figure 42: Comparison of Pressure profiles around the wellbore drawdown region for updated model (considering Diffusion and Desorption) against base model.

5.3 Production Forecast

We observed in last section that the SRV volume from which gas was being drained out was confined to a lower length of the fractures for the same amount of production, against the initial model. Now, a study is done to see how these changes would impact the production. So prediction was made with the model considering diffusion and desorption against the initial model we had started off with. We used 1 year of production data to make forecast for the next 30 years, which is normally the industry practice now, using BHP as the production constraint. Results for cumulative gas production, gas rates at surface condition and average reservoir pressure are shown in figure 43, 44 and 45 respectively.

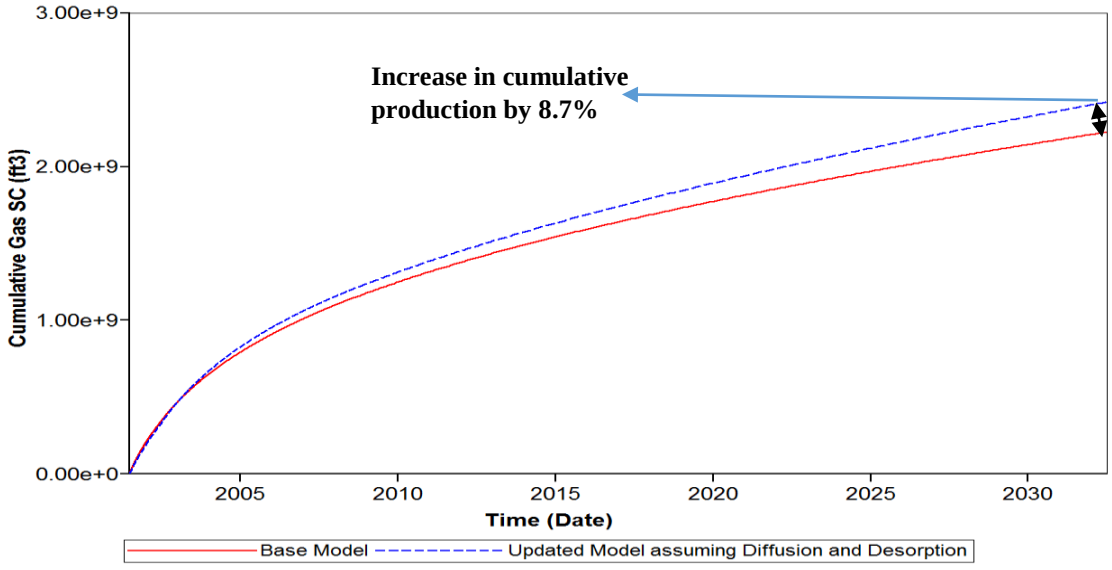

Figure 43 - Production forecast comparing cumulative gas production for base and updated model, produced fed on a BHP constraint.

As expected, we see an increase in production of around 8.7% against the results that were predicted by our base model. Gas rates were up by 18%, with diffusion and desorption helping in the gas drainage capacity of the matrix, at later time of production. The reservoir pressure was down by around 230 psi, mainly because of the diffusion affect. The higher pressure in base case could be explained by the fact that there is still gas left in the nano pores that couldn't be produced.

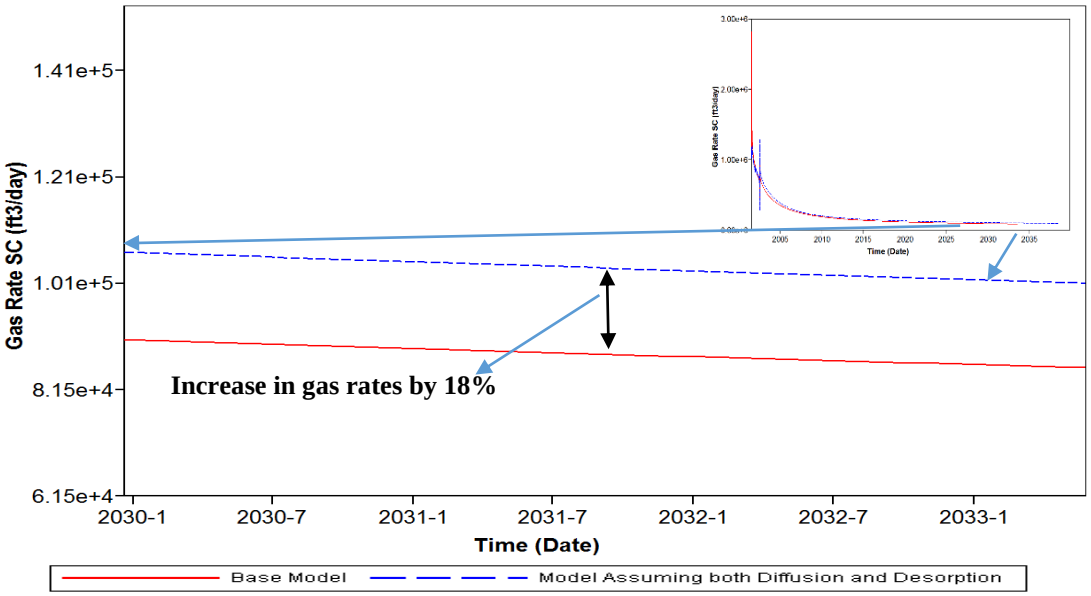

Figure 44 - Production forecast for daily gas rates for base and updated models, produced on a constant BHP.

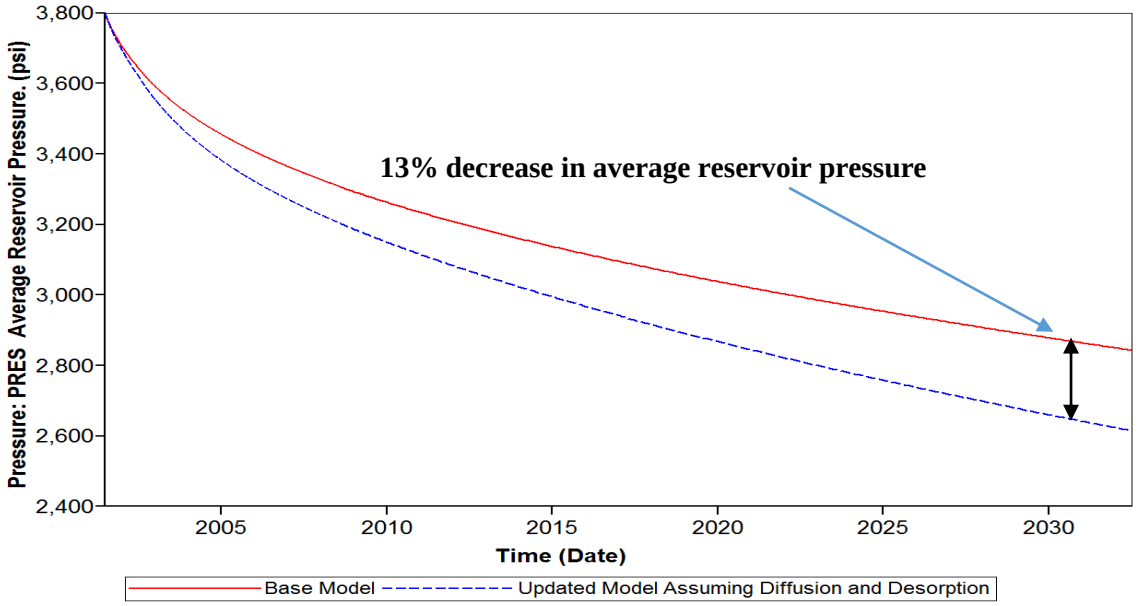

Figure 45- Forecast for average reservoir pressure for base and updated models, produced on a constant BHP.

5.4 Conclusions

After integrating diffusion and desorption in the model, we perform a history match. Parameter selection for this process was based on our results from the sensitivity analysis that considered different petro-physical properties and SRV parameters, and their values were constrained by the ranges found from literature. It was found that the SRV volume contributing towards flow had reduced for the same of production. Predictions made from the updated model showed an increase in production, even at very late time of production because of extra mechanisms helping in the production from the pore network.

CHAPTER VI
DISCUSSION AND CONCLUSIONS

This work focusses on modelling gas flow through shale, by upscaling the assumptions of the physics for flow and details of the porosity system that exist at nano scale level to a reservoir scale. We worked with data of a horizontal well producing gas from Barnett Formation and showed how it could be analyzed using the concept of a micro-scale multi porosity system guided by different mechanisms like Darcy flow, diffusion and desorption, that contribute towards higher production.

It is observed that adsorption is very important for increasing gas in place reserves estimation, but its contribution towards gas production in Barnett Shale is insignificant because of low permeability in matrix. Also, higher TOC values along with higher Langmuir pressures would help in bringing the dominance of desorption process in economic analysis. This was also proved by the analysis of our Monte Carlo simulation results, which showed that our cumulative production only increased by around 11% for high values of TOC observed in Barnett Shale.

Apparent dynamic permeability concept is then used to incorporate the details of Darcy flow, diffusion and transient affect between matrix and fracture from the micro scale model, using rock tables. Results indicate that diffusion helped to maintain gas drainage capacity of the matrix system, where as effects of desorption were mainly observed in the later part of the depletion when the free gas in the system has been used. Modelling of both these processes gives results different from model initially used, because matrix

contribution towards production was found to be greater, which resulted in increased production by around 9% after 30 years simulation run. This ultimately affected our SRV volume, reducing the fracture extension into matrix by around 15%. Thus, we can use these findings to optimize the SRV network to bring the completion costs down, which is a major chunk of our well cost. This will result in completions design using fewer number of hydraulic fractures, for same or even greater production. Similarly, this idea can also be used in the context of effective well spacing for field development.

Further suggestion to carry this work forward could include studying the effect of stresses on the apparent permeability if slit shaped organic micro pores are assumed. This technique can also be used to study the phenomenon of fracture fluid flowback, if field data is available for it.

REFERENCES

Andrade Perdomo, J. F., Civan, F., Devegowda, D., & Sigal, R. F. (2011, January 1). Design and Examination of Requirements for a Rigorous Shale-Gas Reservoir Simulator Compared to Current Shale-Gas Simulator. Society of Petroleum Engineers. doi:10.2118/144401-MS

Bruner, K.R, Richard Smosna (April 2011), A Comparative Study of the Mississippian Barnett Shale,Fort Worth Basin, and Devonian Marcellus Shale, Appalachian Basin – US Department of Energy

Civan, F., Rai, C. S., and Sondergeld, C.H. 2011. Shale-Gas Permeability and Diffusivity Inferred by Improved Formulation of Relevant Retention and Transport Mechanisms , Transport in Porous Media, Vol. 86 (3): 925-944.

Curtis, M.E., Ambrose, R.J., and Sondergeld, C.H. 2010. Structural Characterization of Gas Shales on the Micro- and Nano-Scales. Paper presented at the Canadian Unconventional Resources and International Petroleum Conference, Calgary, Alberta, Canada. Society of Petroleum Engineers SPE-137693-MS. DOI: 10.2118/137693-ms.

Ertekin, T., King, G. A., & Schwerer, F. C. (1986, February 1). Dynamic Gas Slippage: A Unique Dual-Mechanism Approach to the Flow of Gas in Tight Formations. Society of Petroleum Engineers. doi:10.2118/12045-PA

Haghshenas, B., Clarkson, C. R., & Chen, S. (2013, November 5). Multi-Porosity Multi-Permeability Models for Shale Gas Reservoirs. Society of Petroleum Engineers. doi:10.2118/167220-MS

Jarvie, D.M., Hill, R.J., Pollastro, R.M., Claxton, B.L., and Bowker, K.A., 2004, Evaluation of hydrocarbon generation and storage in the Barnett Shale, Fort Worth basin, *in* Barnett Shale and other Fort Worth basin plays, Ellison Miles Memorial Symposium, Ellison Miles Geotechnical Institute, Brookhaven College, TX,p. 2–5.

Jarvie, D.M., Hill, R.J., Ruble, T.E., and Pollastro, R.M., 2007, Unconventional shale-gas systems: the Mississippian Barnett Shale of north-central Texas as one model for thermogenic shale-gas assessment: American Association Petroleum Geologists Bulletin, v. 91, p. 475–499

Javadpour, F., Fisher, D., & Unsworth, M. (2007, October 1). Nanoscale Gas Flow in Shale Gas Sediments. Petroleum Society of Canada. doi:10.2118/07-10-06

Javadpour, F. (2009, August 1). Nanopores and Apparent Permeability of Gas Flow in Mudrocks (Shales and Siltstone). Petroleum Society of Canada. doi:10.2118/09-08-16-DA

Killough, J. E., Wei, C., Liu, H., Yan, B., Qin, G., Wang, H., & Guo, W. (2013, April 19). Characterization and Analysis on Petrophysical Parameters of a Marine Shale Gas Reservoir. Society of Petroleum Engineers. doi:10.2118/165380-MS

Lu, X. C., Li, F. C., and Watson, A. T. 1995 . Adsorption Measurements in Devonian Shales. Fuel , v. 74, pp. 599-603.

Loucks, R. G., Reed, R. M., Ruppel, S. C., and Hammes, Ursula, 2012, Spectrum of pore types and networks in mudrocks and a descriptive classification for matrix-related mudrock pores: AAPG Bulletin, v. 96, no. 6, p. 1071–1098.

Mayerhofer, M. J., Lolon, E., Warpinski, N. R., Cipolla, C. L., Walser, D. W., & Rightmire, C. M. (2010, February 1). What Is Stimulated Reservoir Volume? Society of Petroleum Engineers. doi:10.2118/119890-PA

Mayerhofer, M. J., Lolon, E. P., Youngblood, J. E., & Heinze, J. R. (2006, January 1). Integration of Microseismic-Fracture-Mapping Results With Numerical Fracture Network Production Modeling in the Barnett Shale. Society of Petroleum Engineers. doi:10.2118/102103-MS

Mengal, S.A., and Wattenbarger, R.A. 2011. Accounting for Adsorbed Gas in Shale Gas Reservoirs. Paper SPE 141085, SPE Middle East Oil and Gas Show and Conference , Manama, Bahrain, September 25-26

Montgomery S.L., Jarvie D.M., Bowker K.A. , Pollastro R.M.: "Mississippian Barnett Shale, Fort Worth Basin, North-Central Texas : Gas-Shale Play with Multi-Trillion Cubic Foot Potential" AAPG Bulletin , v.89 , No.2(Feb 2005),pp. 155-175.

Seldle, J.P. and Arri, L.E. 1990. Use of Conventional Reservoir Models for Coalbed Methane Simulation. Paper presented at the Annual Technical Meeting, Calgary, Alberta. Petroleum Society of Canada PETSOC-90-118. DOI: 10.2118/90-118.

Silin, D., and Kneafsey, T., 2012. Shale Gas: Nanometer-Scale Observations and Well Modeling. Journal of Canadian Petroleum Technology, 51 (6): 464–475.

Sing, K.S.W., Everett, D.H., Haul, R.A.W., Moscou, L., Pierotti, R.A., Rouquerol, J., and Siemien-iewska, T., 1985. Reporting Physisorption Data for Gas/Solid Systems with Special Reference to the Determination of Surface Area and Porosity (Recommendations 1984). Pure Appl. Chem. 57 (4): 603–619

Sondergeld, C. H., Newsham, K. E., Comisky, J. T., Rice, M. C., & Rai, C. S. (2010, January 1). Petrophysical Considerations in Evaluating and Producing Shale Gas Resources. Society of Petroleum Engineers. doi:10.2118/131768-MS

Sun, H., Chawathe, A., Hoteit, H., Shi, X., & Li, L. (2015, February 1). Understanding Shale Gas Flow Behavior Using Numerical Simulation. Society of Petroleum Engineers. doi:10.2118/167753-PA

Tongwei Zhang , Geoffrey S. Ellis , Stephen C. Ruppel , Kitty Milliken , Rongsheng Yang :Effect of organic-matter type and thermal maturity on methane adsorption in shale-gas systems : Organic Geochemistry , Volume 47, June 2012, Pages 120–131

Wang, F. P., & Reed, R. M. (2009, January 1). Pore Networks and Fluid Flow in Gas Shales. Society of Petroleum Engineers. doi:10.2118/124253-MS

Wu, P., & Aguilera, R. (2013, November 5). Uncertainty Analysis of Shale Gas Simulation: Consideration of Basic Petrophysical Properties. Society of Petroleum Engineers. doi:10.2118/167236-MS

Yan. B, Y. Wang . J.E Killough , Beyond Dual Porosity Modelling for the Simulation of Complex Flow Mechanisms in Shale Reservoirs : SPE 163651 , 2013

Yan, B., Killough, J. E., Wang, Y., & Cao, Y. (2013, August 12). Novel Approaches for The Simulation of Unconventional Reservoirs. Society of Petroleum Engineers. doi:10.1190/URTEC2013-131

Yan, B., Alfi, M., Wang, Y., & Killough, J. E. (2013, September 30). A New Approach for the Simulation of Fluid Flow In Unconventional Reservoirs Through Multiple Permeability Modeling. Society of Petroleum Engineers. doi:10.2118/166173-MS

Yu, W., Sepehrnoori, K., & Patzek, T. W. (2014, October 27). Evaluation of Gas Adsorption in Marcellus Shale. Society of Petroleum Engineers. doi:10.2118/170801-MS

APPENDIX A

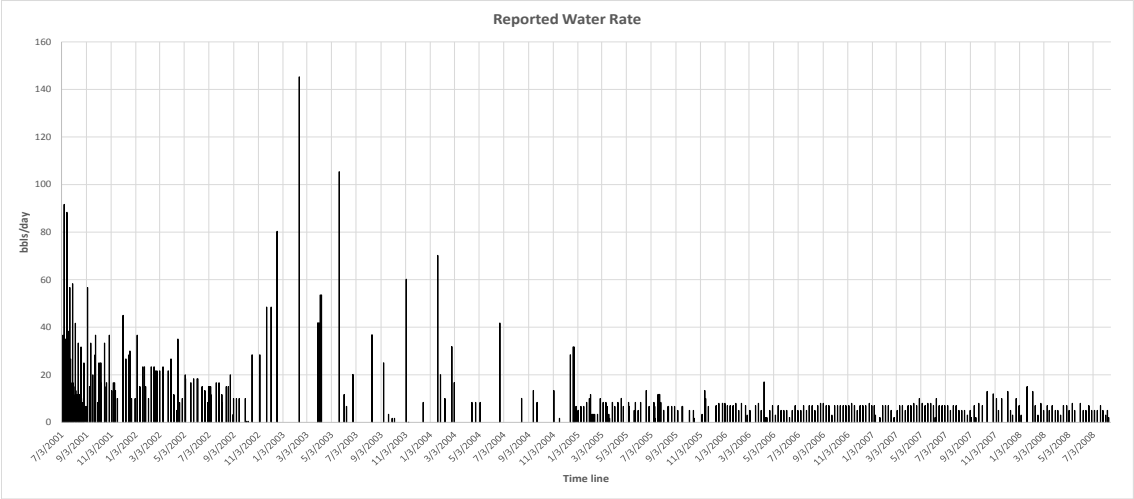

Figure 46: Daily Water Production Rates from the production data.

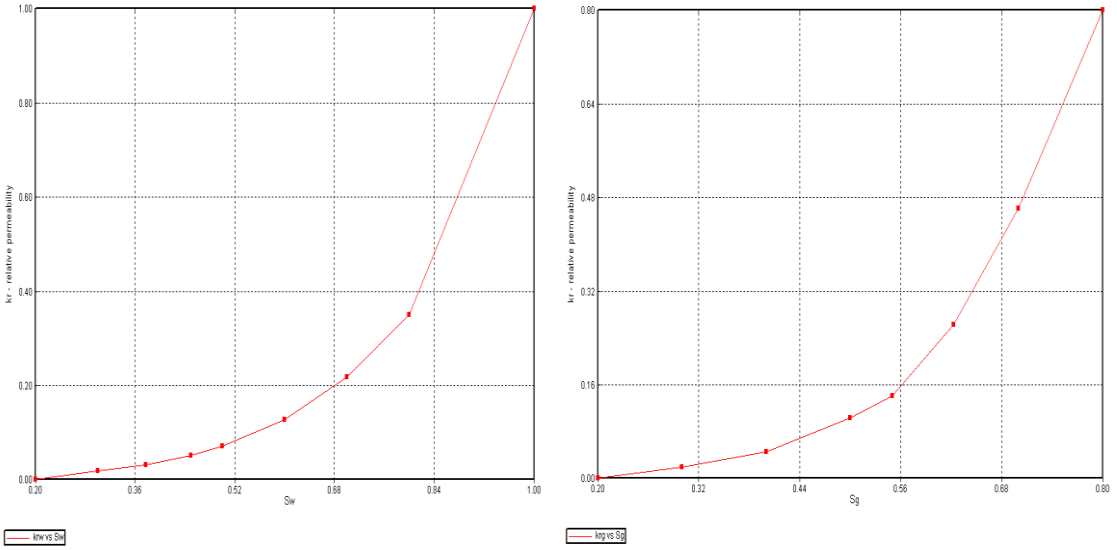

Figure 47 Relative Permeability curves for the matrix part of the model.

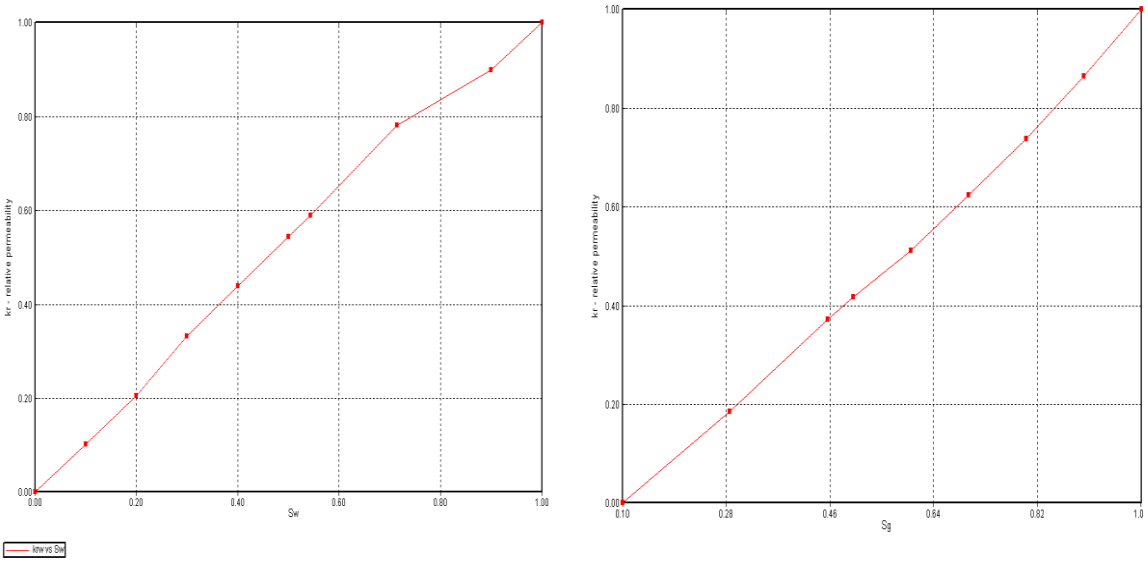

Figure 48 Relative Permeability curves for the fracture (natural + hydraulic) part of the model.

Table 5 - Comparing results of our history match against the initial model, for parameters that were allowed to vary.

Parameters	**New Value after History Match (Assuming Diffusion & Desorption)**	**Old Value (Without Assuming Diffusion & Desorption)**
Matrix Permeability, mD	0.0001	0.0000765
Hydraulic Fracture Permeability, mD	127.5	127.5
Natural Fracture Permeability (Set 1), mD	0.09	1.01
Natural Fracture Permeability (Set 2), mD	51	56.6
TOC, wt%	4	Not Assumed
Minimum BHP for Operating Conditions, Psi	375	320
Matrix Porosity	5.1	6.7
Rock Density, lbm/scf	164.2	Not Assumed
length of Natural Fractures (N-E), ft	1000	840
length of Natural Fractures (S-W), ft	2000	1820